Lognormal Mixture Model for Option Pricing with Applications to Exotic Options

by

Mingyu Fang

A thesis
presented to the University of Waterloo
in fulfillment of the
thesis requirement for the degree of
Master of Mathematics
in
Actuarial Science

Waterloo, Ontario, Canada, 2012

I hereby declare that I am the sole author of this thesis. This is a true copy of the thesis, including any required final revisions, as accepted by my examiners.

I understand that my thesis may be made electronically available to the public.

Abstract

The Black-Scholes option pricing model has several well recognized deficiencies, one of which is its assumption of a constant and time-homogeneous stock return volatility term. The implied volatility smile has been studied by subsequent researchers and various models have been developed in an attempt to reproduce this phenomenon from within the models. However, few of these models yield closed-form pricing formulas that are easy to implement in practice. In this thesis, we study a Mixture Lognormal model (MLN) for European option pricing, which assumes that future stock prices are conditionally described by a mixture of lognormal distributions. The ability of mixture models in generating volatility smiles as well as delivering pricing improvement over the traditional Black-Scholes framework have been much researched under multi-component mixtures for many derivatives and high-volatility individual stock options. In this thesis, we investigate the performance of the model under the simplest two-component mixture in a market characterized by relative tranquillity and over a relatively stable period for broad-based index options. A careful interpretation is given to the model and the results obtained in the thesis. This differentiates our study from many previous studies on this subject.

Throughout the thesis, we establish the unique advantage of the MLN model, which is having closed-form option pricing formulas equal to the weighted mixture of Black-Scholes option prices. We also propose a robust calibration methodology to fit the model to market data. Extreme market states, in particular the so-called crash-o-phobia effect, are shown to be well captured by the calibrated model, albeit small pricing improvements are made over a relatively stable period of index option market. As a major contribution of this thesis, we extend the MLN model to price exotic options including binary, Asian, and barrier options. Closed-form formulas are derived for binary and continuously monitored barrier options and simulation-based pricing techniques are proposed for Asian and discretely monitored barrier options. Lastly, comparative results are analysed for various strike-maturity combinations, which provides insights into the formulation of hedging and risk management strategies.

Acknowledgements

I would like to express my utmost thanks to my supervisor, Professor Tony Wirjanto, for his guidance, support, and care throughout the completion of this thesis. I would also like to thank Professor Chengguo Weng and Professor Adam Kolkiewicz for their kind suggestions that facilitate the progress in bringing this thesis to its completion.

Dedication

This thesis is dedicated to my parents and loved ones.

Table of Contents

List of Tables vii

List of Figures viii

1 Introduction 1

2 Review of the Black-Scholes Framework 4

2.1 The Black-Scholes Formula 4

2.2 The Volatility Smile 7

3 Lognormal Mixture Model for European Option Pricing 11

3.1 The Mixed Diffusion Process for Stock Prices 12

3.2 The Lognormal Mixture Model 15

3.2.1 Model Specifications 15

3.2.2 Option Greeks and Hedging 19

3.2.3 Dynamics of the Two-component Mixture model 24

3.3 Calibration Techniques 28

3.3.1 Data Structure and Calibration Methodology 28

3.3.2 Empirical Results and Analysis 33

3.4 Interpretation of the Mixture Model 41

4 Pricing Exotic Options **44**

4.1 Binary Options 44

4.1.1 A Closed-form Pricing Formula under Mixture Lognormal Model . . 45

4.1.2 Calibration Technique and Empirical Example 47

4.2 Path Dependent Options: Asian Option 48

4.2.1 Pricing Technique with Simulation 50

4.2.2 Pricing Example and Analysis 52

4.3 Path Dependent Options: Barrier Option 56

4.3.1 Pricing Formulas and Simulation-based Pricing Methodology 58

4.3.2 Pricing Example and Analysis 60

5 Conclusion **65**

APPENDICES **67**

A Proof of Proposition 3.1 **68**

B Proof for Proposition 3.2.1 Using Partial Expectations **70**

C Formula for European Option Greeks under Black-Scholes Framework **72**

D Proof for Proposition 3.2.3 **74**

E Formula for Continuously Monitored Barrier Option Prices under Black-Scholes Framework **75**

F Derivation of the Critical Values for CME Entropy **77**

References **78**

List of Tables

3.1 Calculation for example 3.2.2 - component process Greeks 22
3.2 Calculation for example 3.2.2 - option Greeks under the MLN model 23
3.3 Summary of call option data used for calibration 34
3.4 Fitted parameters for the MLN model and Black-Scholes model 35
3.5 Estimated crash-o-phobia parameters of selected times to maturity 36
3.6 Performance of fitted MLN and Black-Scholes models for European call . . 37

4.1 Performance of fitted MLN and Black-Scholes models for binary call 48
4.2 Performance of MLN and Black-Scholes models for Asian call 54
4.3 Performance of MLN and Black-Scholes models for continuous barrier call . 62
4.4 Performance of MLN and Black-Scholes models for discrete barrier call . . 63

C.1 Black-Scholes formulas for option Greeks 72

E.1 Black-Scholes formulas for continuously monitored barrier options 76

List of Figures

2.1 Volatility surface of S&P500 index options for March 1999 9

3.1 Results for call option pricing, percentage error vs. spot-strike difference . 37
3.2 Implied volatility under MLN for call option maturing in 32 days 39
3.3 Comparative result of implied volatility smiles 40
3.4 Implied volatility smiles under varying MLN volatility combinations 41

4.1 Results for binary option pricing, percentage error vs. spot-strike difference 49
4.2 APAC price differences under MLN and BS models, fixed maturity 55
4.3 C_{DI} price differences under MLN and BS models, fixed maturity 64

Chapter 1

Introduction

The Black-Scholes option pricing model (1973)[2] is the most commonly used model in the financial market for European style stock option pricing. It has subsequently been expanded by researchers to build models that can price various forms of financial derivatives. Basically, the model assumes that the stock price follows a Geometric Brownian Motion with constant drift and volatility terms, which is represented statistically by a conditional lognormal distribution. Deficiency of this assumption has been studied theoretically and empirically by researchers, where the phenomenon of implied volatility smile/skew presents a particular challenge to the model. This phenomenon describes how the volatility embedded in the true market price of an option varies with its strike price and term to maturity. The volatility smile phenomenon contradicts the volatility assumption underlying the Black-Scholes model since the implied volatility in the Black-Scholes model is time invariant. In fact, true stock return volatility is notoriously known for its time-varying nature and stylized patterns, which is not captured by the Black-Scholes model. Potential causes of the volatility smile have been a subject much studied in the literature, and this thesis contributes further to this line of research as well.

While many models and techniques have been developed over the years in an effort to explain the volatility smile phenomenon, none of them provide closed-form expressions for option prices similar to the ones in the traditional Black-Scholes model. In addition, the complexity of these models make their implementations in practice far from being straightforward. Examples of this include the GARCH option pricing model proposed by Duan (1995)[13]. In addition, some of the prior studies also employ models that lack a formal interpretation of their specifications and results. In this thesis, we present a Mixture Lognormal option pricing model (MLN), where the stock price path is described by a mixture

of conditional lognormal distribution. This model not only results in Black-Scholes style formulas for European options that are easy to implement, but also generates volatility smiles that are consistent with much of the empirical evidence.

MLN models are recently studied by Brigo et al. (2002)[4], who examined some of the theoretical properties of the mixture lognormal distribution in producing desired volatility smiles. Empirical examples are given by Brigo (2002) using interest rate options and individual stock options under a three-component mixture model. The ability to produce volatility smiles is then tested under a hypothetical setting. Leisen (2003)[28] specified a more general MLN model where the component drifts vary and studied its property as an approximation to jump-diffusion and stochastic volatility models. Neumann (2002)[35] discussed the two-component mixture model and obtained empirical insights on its application to German broad-based stock index options during a period characterized by turbulences and high volatility in the markets.

Our MLN model incorporates the major advantages of the previous specifications. In the implementation part, we propose a least-square calibration methodology that best yields the optimal parameter estimates. Empirical results are validated using a two-component mixture model. However, we focus on the application to broad-based index options during a relatively tranquil and low-volatility period, which differs from the setting in most previous empirical studies. The objective of this chosen period is to investigate the pricing performance of our two-component MLN model versus the traditional Black-Scholes model under the most unfavourable condition for the MLN framework and the most favourable condition for the Black-Scholes framework. The ability of the two-component MLN model in generating volatility smiles under different settings is carefully examined. As a major contribution of this thesis, we extend the model to exotic stock options, for which closed-form formulas are derived and simulation-based pricing methods are devised and implemented. Comparative results are also presented in this thesis to highlight the unique features of our MLN framework.

The rest of the thesis is organized as follows: Chapter 2 provides a review of the Black-Scholes framework and discusses the nature of the volatility smile phenomenon. For completeness, results obtained in previous studies are also discussed. Chapter 3 specifies our MLN model, which starts from the derivation of the mixture diffusion process as well as the mixture lognormal framework for stock prices. We prove theorems that most option quantities under the MLN model are linear mixtures of the ones under the Black-Scholes model, which leads to closed-form pricing formulas. Hedging is briefly discussed and the two-component mixture is studied in detail equipped with a careful interpretation of the

results in this chapter. Empirical result is presented based on closing S&P500 index option quotes. Chapter 4 provides detailed derivation of pricing formulas/techniques for exotic derivatives, which include binary, Asian, and barrier options. Empirical examples are also provided under semi-hypothetical settings that are intended to serve for illustrative purpose only. Chapter 5 provides the conclusion and summary of our major findings for this thesis. To avoid confusion, all propositions and definitions are numbered at the subsection level while all equations, tables, and figures are numbered at the chapter level. Consistent notations are used throughout the presentation and important definitions are conveniently catalogued in this thesis.

Chapter 2

Review of the Black-Scholes Framework

2.1 The Black-Scholes Formula

An option pricing model introduced by Black and Scholes (1973)[2] provides a fundamental framework for the pricing of European style options. Subsequently this framework has been extended to more complicated pricing models for various derivatives including exotic options. The basic specifications of the model rely on the assumption that the price of the underlying asset follows a lognormal distribution with constant mean and time-invariant volatility. For simplicity and without loss of generality, we review key attributes of the model on a single European stock option. In particular, we emphasize major deficiencies of the model that have constituted the focus of various researches and published literatures in finance.

Let (Ω, F, P) denote a properly defined probability space and let $t \in [0, T]$ denote the time, where T is the time to maturity of the option. Then, a stock price, denoted by $S(t)$, is assumed to be generated by the a one-dimensional time-homogeneous diffusion process:

$$\frac{dS(t)}{S(t)} = \mu dt + \sigma dZ(t), \tag{2.1}$$

where μ is the drift term, σ is the volatility or diffusion term and $Z(t)$ is the standard Brownian Motion.

Solving this stochastic differential equation with the initial condition:

$$S(0) = S_0,$$

where S_0 denotes the stock price at the beginning of the time frame, yields the following result (Black and Scholes[2]):

$$S(t) = S_0 e^{(\mu - \frac{1}{2}\sigma^2)t + \sigma\sqrt{t}Z(t)}, \tag{2.2}$$

Notice that both the instantaneous mean return μ and volatility σ are assumed to be time-invariant. Under a risk neutral measure Q (and hence a forward measure), the risk free rate is used as a discount rate to obtain an arbitrage-free price of an asset. This translates equation (2.2) into its equivalence under the risk neutral measure probability space (Ω, F, Q) that guarantees no arbitrage:

$$S(t) = S_0 e^{(r - \delta - \frac{1}{2}\sigma^2)t + \sigma Z(t)}, \tag{2.3}$$

where:

1. r is the continuously compounded risk free rate
2. δ is the continuously paid dividend rate

Since $Z(t)$ is a standard Brownian motion, it has a Normal $(0, t)$ distribution and therefore the stock price follows a lognormal distribution:

$$S(t) \equiv LN(\ln S_0 + (r - \delta - \frac{1}{2}\sigma^2)t, \sigma\sqrt{t}). \tag{2.4}$$

For a derivation of the option prices, it is useful to define the following statistical term, which will be used in later discussions as well.

Definition 2.1: *Let X be a continuous random variable valued in R^+ with a density function $f_X(x)$ and a distribution function $F_X(x)$. A Partial Expectation of X truncated from below at constant K, denoted by $PE_K^+(x)$, is the contribution to the expected value of X bounded from below by K*

$$PE_K^+(x) = \int_K^\infty x f_X(x) dx, \tag{2.5}$$

and the Partial Expectation of X truncated from above at constant K, denoted by $PE_K^-(x)$, is defined accordingly:

$$PE_K^-(x) = \int_0^K x f_X(x) dx, \tag{2.6}$$

A European Call option with a strike price K on a stock currently priced at S_0 has a payoff at maturity time $T : (S(T) - K)^+$ and its expected discounted value is the arbitrage-free price proposed by Black and Scholes (1973)[2] under the risk neutral measure, which we denote by $C_{BS}(S_0, K, T, r, \delta)$:

$$\begin{aligned} C_{BS} &= E^Q[(e^{-rT}(S(T) - K)^+] \\ &= e^{-rT} E^Q[(S(T) - K)^+] \\ &= e^{-rT} E^Q[S(T) - K \mid S(T) > K] Q(S(T) > K) \\ &= e^{-rT}[PE_K^+(S(T)) - KQ(S(T) > K)]. \end{aligned} \tag{2.7}$$

According to the lognormal distributional relationship in equation (2.4) for the stock price, the following result is obtained[2]:

$$PE_K^+(S(T)) = S_0 e^{r-\delta} N(d_1), \tag{2.8}$$

$$Q(S(T) > K) = N(d_2). \tag{2.9}$$

where, $N(\cdot)$ represents the standard Normal distribution function and

$$d_1 = \frac{\ln(\frac{S_0}{K}) + (r - \delta + \frac{1}{2}\sigma^2)T}{\sigma\sqrt{T}}, \tag{2.10}$$

$$d_2 = \frac{\ln(\frac{S_0}{K}) + (r - \delta - \frac{1}{2}\sigma^2)T}{\sigma\sqrt{T}} = d_1 - \sigma\sqrt{T}. \tag{2.11}$$

This gives the famous closed-form formula for a European call option price upon substitution into equation (2.7):

$$C_{BS}(S_0, K, T, r, \delta) = S_0 e^{-\delta T} N(d_1) - K e^{-rT} N(d_2). \tag{2.12}$$

To avoid redundancy, in this review, we will focus our discussions on call options only.

However, the derivation for put option prices is relatively straightforward using the put call parity condition. Let P_{BS} denote the Black-Scholes price for a put option with maturity T and strike price K, it is easy to obtain the following result:

$$P_{BS}(S_0, K, T, r, \delta) = Ke^{-rT}N(-d_2) - S_0e^{-\delta T}N(-d_1). \tag{2.13}$$

The above closed-form option pricing formulas conclude the review of the main results in the Black-Scholes model. Notice that under the risk neutral measure both the discount rate and volatility are constants. In reality, discount rates are better modelled by stochastic processes. Stochastic Discount Factor Models under exponential-affine forms are studied in Gourieroux and Monfort(2006)[16], and Jacobs and Karoui (2009)[25]. This will not be the focus of the thesis although admittedly, the Volatility Skew (Smile) phenomenon can be partially attributed to this factor.

2.2 The Volatility Smile

While the Black-Scholes pricing formula for options is appealing in practice for their simplicity and ease of implementation, several of its shortcomings of have been put under intense scrutiny by academic researchers and financial professionals.

First of all, the risk neutral densities of most stock index returns have generally displayed negative skewness and leptokurtosis, as documented in Corrado and Su (1996) using the S&P500 index from 1926 to 1995[10]. Individual stock returns are also found to be less negatively skewed and present more variations as shown in Bakshi, Kapadia and Madan (2003)[1]. Many models have been developed to accommodate these deviations from Gaussian moments, including the use of Skewness and Kurtosis Adjusted Black-Scholes model derived from density expansions by Corrado and Su (1997)[11] and Brown and Robinston (2002)[5], Generalized Extreme Value Distribution (GEV) proposed by Markose and Alentorn (2005)[31] and exponential Lévy's Processes discussed in Shoultens and Symens (2003)[39].

Secondly, volatilities of stock returns are observed to be ubiquitously time-varying and heteroscedastic. Efforts directed to account for this include the stochastic volatility models by Hull and White (1987)[23] and Heston (1993)[22], the pricing method by Dupire (1994)[14] derived from Fokker-Planck equations, and econometric models incorporating GARCH-type conditional volatility processes by Engel and Mustafa (1992)[15] and Duan(1995)[13].

The goal of the aforementioned studies is to generate the volatility smiles observed in option markets. This is also our aim by using a novel lognormal mixture model. To this end, we first define the implied volatility of an option as follows:

Definition 2.2: *The implied volatility of an option, denoted by σ_{im}, is the volatility implicitly assumed so that the option's Black-Scholes price is equal to its market price denoted by C_m. For an European call option, it is implicitly defined by the following relationship,*

$$C_m(S_0, K, T, r, \delta) = C_{BS}(S_0, K, T, r, \delta), \tag{2.14}$$

or, in expanded form, by

$$C_m = S_0 e^{-\delta T} N\left(\frac{\ln\left(\frac{S_0}{K}\right) + \left(r - \delta + \frac{1}{2}\sigma_{im}^2\right)T}{\sigma_{im}\sqrt{T}}\right) - Ke^{-rT} N\left(\frac{\ln\left(\frac{S_0}{K}\right) + \left(r - \delta - \frac{1}{2}\sigma_{im}^2\right)T}{\sigma_{im}\sqrt{T}}\right) \tag{2.15}$$

This makes it clear that solving for the implied volatility from market option prices requires numerical procedures except for the ideal case where the option is at the money (ATM) and the underlying stock has a continuous dividend rate equal to the risk free rate (e.g. $r = \delta$). When this situation approximately holds, equation (2.15) can be substantially simplified.

If the Black Scholes Framework holds in the real market, the implied volatility should remain constant and invariant with respect to other option terms such as time to maturity T and strike price K. This is generally not the case in the real world. Empirical evidence (see Daglish, Hull, and Suo (2006)[12]) shows that for options of a specific stock with a certain time to maturity, implied volatility are lowest when the option is at the money. Plots of implied volatility vs. strike price (or moneyness defined as K/S) usually reveals volatility skewness in the shape of smiles.

In addition, the implied volatilities vary for otherwise identical options with different times to maturity. This is known as the term structure of implied volatilities. A three dimensional representation, referred to as the volatility surface, can thus be created showing the changes in implied volatility with respect to both strike price (or moneyness) and time to maturity (See Figure 2.1 below, which is reproduced from Cont and da Fonseca (2002)[9]).

The volatility surface predicted by the Black-Scholes framework should be a flat and horizontal plane in theory, which is contradicted by the empirical stylized fact.

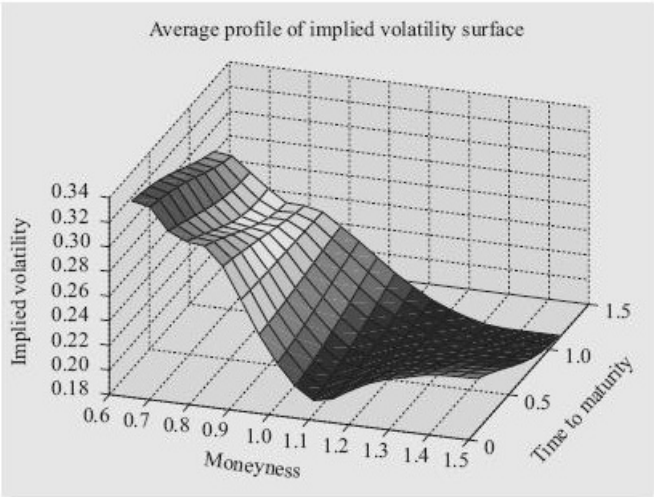

Figure 2.1: Volatility surface of S&P500 index options for March 1999

The cause of the volatility smile phenomenon remained unclear until a series of findings reported in studies that emerged in the literature. Following the pioneering study on the calculation of implied volatility smiles by Chiras and Manaster (1978)[8], research has been attempted to explain volatility smile by appealing to market imperfections in the form of transaction costs. In the absence of arbitrage opportunities, the time-t price S_t of any security within the time frame of interest $t \in [0, T]$ equals its discounted expected terminal value S_T with respect to the equivalent martingale measure Q:

$$S_t = E_t^Q[S_T e^{-r(T-t)}]. \tag{2.16}$$

This is consistent with the risk neutral pricing approach in our previous review of the Black-Scholes Model, where the equivalent martingale measure is replaced by a unique risk-neutral measure (Ω, F, Q).[1]. Using the martingale restriction test, Longstaff (1995)[30] confirms that both implied volatilities and implied underlying stock price (and hence moneyness as in Figure 2.1) from the lognormal models almost always exceed the true values.

[1]We will continue to use the risk-neutral methodology in our future derivations. The rationale for this is discussed in Harrison and Kreps (1979)[19], and Harrison and Pliska (1981)[20].

The rationale is that due to transaction costs, the replicating portfolio of any security is more expensive than the security. Regressions of the price differences reported by Longstaff (1995) on the bid ask spread indicate that this interpretation constitutes at least one of the causes. However, transaction costs are nearly constant over time, meaning that the generated Black-Scholes volatility term should be level over time as well. This is apparently contradicted by empirical findings. Jackwerth and Rubinstein (1996)[38] showed that the volatility changed structurally during the 1987 market crash, which cannot be captured by the lognormal distribution implicit in the Black-Scholes framework. In addition, the probability distribution of stock returns calculated using Rubinstein's method (1994)[37] revealed a fat left tail and excess skewness. This density cluster of extreme loss events, which is referred to as a crash-o-phobia phenomenon[2], cannot be modelled by the Black-Scholes specifications.

Therefore, the crash-o-phobia phenomenon serves as a major, if not conclusive, cause for the implied volatility smile/surfaces observed in the real market as it cannot be properly captured by the lognormal stock price model under the Black-Scholes framework. As pointed out by Neumann (2002)[35], Melick and Thomas(1997)[32] report similar problems using American oil futures options during the Gulf crisis. They also extend the effort to show that a mixture of lognormal distributions is able to represent the crash-o-phobia phenomenon and leads to better oil future option prices than the Black-Scholes model empirically. This finding enlightens subsequent researches on mixture models in solving smile related problems, which constitutes the topic of our study.

In summary, studies on implied volatilities were abundant in the literature and presented serious challenges to the efficacy of the traditional Black-Scholes option price model. Apparently, the existence of volatility smile makes the empirical application of Black-Scholes formula questionable. Studies mentioned previously provide solutions to the volatility smile phenomenon. However, most of them do not provide closed-form pricing formulas like the ones in the original Black-Scholes framework. In fact, one of the key advantages of the lognormal mixture model is its ability to provide Black-Scholes style option pricing formulas that are easy to implement. In the next chapters, we will present this model in general as well as in its most basic form, propose calibration procedures, and extend its application to exotic options.

[2]Literally, the term refers to the market's general fear of downside risk upon experience of extreme events. However, it involves additional elements under the context of implied parameters and option pricing, which will be briefly explained in Section 3.2.3.

Chapter 3

Lognormal Mixture Model for European Option Pricing

As introduced in the previous section, the volatility skew/smile is both evidence and result of the deficiencies in the original Black-Scholes framework. Most of the methods adapted in the studies mentioned earlier rely on the ad-hoc inclusion and adaptation of external model families to generate a desired theoretical level of negative skeweness, leptokurtosis, jumps, and volatility clusters in stock returns. Though some of these methods have been proven to be quite successful, they are often introduced at an increasing cost. For instance, individual equities usually display more variability in returns where positive skewness is occasionally observed (Bakshi, Kapadia and Madan (2003)[1]). Applying one of the techniques to price options of individual stocks may not produce the ideal effect as hypothesized.

In this chapter, we present a basic Lognormal Mixture Model for European option pricing leveraging on the established idea that stock prices (approximately) follow a lognormal distribution conditioning on known information. This model improves on the Black-Scholes model in its ability to produce implied volatility smiles that are consistent with empirical market evidence. It also has the advantage over the previously mentioned approaches in the simplicity of its pricing formula: a closed form Black-Scholes Style formula that is easy to implement for both investment and hedging purposes

3.1 The Mixed Diffusion Process for Stock Prices

We start from diffusion processes as we did for the review conducted in Chapter 1. There are different versions of the model of mixed diffusion processes for stock returns proposed by researchers that vary in their assumptions about the underlying stochastic paths followed by the stock price. Notably, Brigo and Mercurio (2001)[4] assume that component diffusion processes of the mixture share the same constant drift term but different time-varying volatility terms. The advantage of the restriction of a common drift is that under certain regularity conditions, a mixture process followed by the stock price has a nice closed form expression for the volatility term as a function of the volatilities of component processes. The derivation for this result relies on the existence of a parametric risk neutral distribution (and hence risk neutral measure) and the dynamics are quite similar to the one adopted by Dupire (1994)[14]. Other studies propose a general approach where drifts vary among component diffusion processes (See Leisen (2003)[28] and Leisen (2004)[29]). In fact, this variation has no effect for the resultant pricing formula under the risk neutral measure. Following these studies, we propose a new specification of the model.

Under a properly defined probability space (Ω, F, P) and time frame of interest $t \in [0, T]$, the stock price is assumed to follow the following one dimensional stochastic process:

$$dS(t) = \mu S(t)dt + \sigma(S(t), t)S(t)dZ(t), \tag{3.1}$$

with an initial condition:

$$S(0) = S_0,$$

where μ is the drift term, $\sigma(S(t), t)$ is the volatility term, and $Z(t)$ is the standard Brownian Motion. Notice that the volatility term is time varying and usually referred to as the local volatility. For generality, it is also assumed to be a deterministic function of the stock price. In order to ensure the existence of a unique strong solution to this SDE, Brigo and Mercurio[4] propose that the following linear growth regularity condition must hold uniformly in t for a suitable $L \in R^+$:

$$\sigma^2(S, t)S^2 \leq L(1 + S^2), \tag{3.2}$$

which is assumed to be satisfied almost surely in our case as we consider bounded time intervals only.

In the same probability space, consider N independent one-dimensional time-homogeneous diffusion processes:

$$dS_i(t) = \mu_i S_i(t)dt + \sigma_i S_i(t)dZ(t),\ i \in 1, 2...N, \tag{3.3}$$

with the common initial condition:

$$S_i(0) = S_0,\ i \in 1, 2...N.$$

The volatilities of the component processes are constants consistent with the assumption of the Black-Scholes framework and thus the regularity condition in equation (3.2) is satisfied trivially. It is not necessary to introduce additional complexity to those processes as the mixture of component volatilities behaves well enough to generate the dynamics of implied volatility smile in the option pricing context, which will be shown later. The problem remained now is the construction of the mixed diffusion process, which requires that we solve for the local volatility term $\sigma(t, S(t))$ in equation (3.1)

Under the same probability space, let $f(s,t)$ denote the density function of $S(t)$ in equation (3.1) and $f_i(s,t)$ denote the density function in equation (3.3). We want to find an expression for $\sigma(t, S(t))$ such that the following result holds:

$$\frac{d}{ds}P(S(t) \leq s) = f(s,t) = \sum_{i=1}^{N} \lambda_i \frac{d}{ds}P(S_i(t) \leq s) = \sum_{i=1}^{N} \lambda_i f_i(s,t),\ i \in 1, 2...N, \tag{3.4}$$

where each $\lambda_i \in (0,1)$ represents a mixture weight for its corresponding component process, meaning that:

$$\sum_{i=1}^{N} \lambda_i = 1,\ i \in 1, 2...N. \tag{3.5}$$

The solution to a less general problem is provided by Brigo and Mercurio (2001)[4], who impose the restriction of equal component diffusion drifts. We extend this theorem and provide the proof in Appendix A.

Proposition 3.1: *Under a mixture diffusion framework defined by equation (3.1) to equation (3.5), assume that the condition of equal drifts is satisfied,*

$$\mu = \mu_i,\ \forall i \in 1, 2..N$$

Then, the local volatility term in equation (3.1) can be expressed as follows:

$$\sigma(S(t),t) = \sqrt{\frac{\sum_{i=1}^{N} \lambda_i \sigma_i^2 f_i(S(t),t)}{\sum_{i=1}^{N} \lambda_i S(t)^2 f_i(S(t),t)}} \tag{3.6}$$

This proposition uniquely characterizes a mixture diffusion process whose component processes are described by equation (3.3). By simple substitution of the result into equation (3.1), the stochastic path followed by the stock is described by the following:

$$dS(t) = \mu S(t) + \sqrt{\frac{\sum_{i=1}^{N} \lambda_i \sigma_i^2 f_i(S(t), t)}{\sum_{i=1}^{N} \lambda_i S(t)^2 f_i(S(t), t)}} S(t) dZ(t). \tag{3.7}$$

Notice that the proposition applies almost surely under the risk neutral measure where the risk free rate dominates. At the same time, the generality of a mixture models is preserved as the density functions are not specified. The lognormal density is chosen in this case (as implied by equation (3.3)) for its simplicity and consistency with most established option pricing frameworks. However, future research using other density functions, such as a Student's t distribution, is encouraged. In fact, option pricing models based on the t-distribution and its extensions have been developed in an effort to take advantage of their extra kurtosis and modified skewness to more accurately described stock returns (see Cassidy et al. (2010)[6]).

In addition, volatility models can also be accommodated to some extent when component volatilities are treated as deterministic functions independent of the price processes. Some proper averaging or simulation techniques can be used when the models are stochastic. In these cases, the volatilities are no longer calibrated in the mixture model. Discretization procedure is also required for this purpose so that the volatilities used are integrals over the desired periods of time. For example, over the period $[0, t_1]$, we may have:

$$\sigma_i = \int_0^{t_1} \sigma_i(t) dt \tag{3.8}$$

The effect of the incorporation of volatility models is not part of our study and we mention it here for illustrative purposes only. The possibly infinite number of component processes brings both flexibility and challenge to us in working with this model. In principle, more mixing processes is expected to yield better fits for the model. At the same time, more effort has to be spent for the calibration of parameters, which adds considerably to the required computational costs. It is thus desirable to use just as many component processes as it is required. Fortunately, a few components are usually enough to capture the volatility smiles, as we will demonstrate later by focusing on the two-component mixture model.

3.2 The Lognormal Mixture Model

In this section we specify the Lognormal Mixture Model, which is simply an extension of the mixture diffusion process discussed previously. We assume that the density function of the stock price process is that of a lognormal distribution conditioning on the most recent information. This is to say, under the probability space (Ω, F, P), we have for each component process:

$$S_i(t) \mid F_{t^-} \equiv LN\left(\ln S_i(t^-) + \left(\mu_i - \frac{1}{2}\sigma_i^2\right)(t - t^-), \sigma_i\sqrt{t - t^-}\right),$$

or, equivalently,

$$f_i(S,t) = \frac{1}{\sqrt{2\pi}S\sigma_i t}\exp\left\{-\frac{\left(\ln\frac{S}{S_0} - \mu_i t + \frac{1}{2}\sigma_i^2 t\right)^2}{2\sigma_i^2}\right\},\ i \in 1, 2..N \tag{3.9}$$

While it is desirable to work backwards from this equation and Proposition 3.1 to derive pricing a formula for some derivatives, it is not necessary for European stock option pricing. Base on the mixture diffusion framework in the previous section and equation (3.9), we can specify a parametric model directly. Nevertheless, the diffusion processes themselves serve as the fundamental elements of the model and thus must be considered in the derivation and application of any mixed-distributional derivative pricing model.

3.2.1 Model Specifications

We claim that a positive continuous random variable follows a Mixture Lognormal (MLN) distribution according to the following definition:

Definition 3.2.1: *Under the probability space (Ω, F, P), let C denote the underlying discrete state variable taking values on $\{i \mid i \in 1, 2, ...N\}$ with $P(C = i) = \lambda_i$. Also, define binary indicator variables $1_{C=i}$, which take the value of 1 if $C = i$ and 0 otherwise. A random variable Y follows a Mixture Lognormal distribution (MLN) iff*

$$Y = \sum_{i=1}^{N} 1_{C=i} X_i,$$

where the X_i are independent lognormal random variables with density functions:

$$f_{X_i}(x; m_i, \sigma_i) = \frac{1}{\sqrt{2\pi} x v_i} \exp\left\{ -\frac{(\ln x - m_i)^2}{2v_i^2} \right\},\ i \in 1, 2...N..$$

In addition, let $\Lambda \in R^N, M \in R^N$[1], and $V \in R^N$ be vectors of the weight parameters λ_i, the mean parameters m_i, and the standard deviation parameters v_i, $i \in 1, 2...N$ respectively. We denote the parametric distributional relationship of Y as follows:

$$Y \equiv MLN(\Lambda, M, V)$$

The cumulative distribution and probability density functions of Y, denoted by $F_Y(y)$ and $f_Y(y)$, directly follow from the above definition:

$$\begin{aligned} F_Y(y) = P(Y \le y) &= P(\sum_{i=1}^{N} 1_{C=i} X_i \le y) \\ &= \sum_{j=1}^{N} P(\sum_{i=1}^{N} 1_{C=i} X_i \le y \mid C = j) P(C = j) \\ &= \sum_{j=1}^{N} P(X_j \le y) P(C = j) \\ &= \sum_{i=1}^{N} \lambda_i F_{X_i}(y), \end{aligned} \tag{3.10}$$

and

$$\begin{aligned} f_Y(y) = \frac{d}{dy} F_Y(y) &= \frac{d}{dy} \sum_{i=1}^{N} \lambda_i F_{X_i}(y) \\ &= \sum_{i=1}^{N} \lambda_i f_{X_i}(y). \end{aligned} \tag{3.11}$$

[1]Here we have used m and v to denote the mean and standard deviation parameter, which is traditionally denoted by μ and σ for lognormal distributions. We did so to avoid confusion with the drift and volatility terms denoted by μ and σ earlier for diffusion processes. In fact, from the Black-Scholes framework in Chapter 1, we know that $m = \ln S_0 + (\mu - \delta - \frac{1}{2}\sigma^2)(T - t)$ and $v = \sigma\sqrt{T - t}$) for stock price processes and distributions at time t.

The results are just as we expect for mixture distributions.

For each component stock price process, we know from the Black-Scholes framework that the price $S_i(t)$ is a lognormal random variable given the initial price S_0 while the mean parameter is equal to the dividend and risk adjusted drift term (see equation (2.4)). The MLN model we construct for stock price based on the diffusion mixture assumes that:

$$S(t) = \sum_{i=1}^{N} 1_{C=i} S_i(t),$$

Clearly, $S(t)$ is a MLN random variable by definition and consequentially, we further claim the following:

$$S_T \mid S_0 \equiv MLN\left(\Lambda, 1^N \ln S_0 + UT - 1^N \delta T - \frac{1}{2}\Sigma^2 T, \Sigma\sqrt{T}\right), \tag{3.12}$$

where $1^N \in R^N$ is the vector whose elements are all equal to 1 to make the vector dimensions match and $U \in R^N$ is the vector containing the drift terms. Notice that the initial price and dividend rate are properties of the stock of interest and thus do not vary among the component price processes.

For derivative pricing, we adopt the traditional risk neutral pricing technique to ensure that there is no arbitrage. Under the risk neutral probability measure (Ω, F, Q), the drift terms of component processes are all replaced by the risk free rate r, which is also used to discount the future derivative payoff. The risk free rate is a market element and thus shared by the component price diffusion processes, making the drift terms equal. As a result, Proposition 3.1 applies almost surely. This is the key reason that generality is still preserved under the model by Brigo and Mercurio (2001)[4], which is not directly pointed out in the literature. Our model specification is thus consistent with most published works on this topic. Notice that equation (3.12) can be translated to its equivalence under a risk neutral measure (and hence a forward measure):

$$S_T \mid S_0 \equiv MLN\left(\Lambda, 1^N \ln S_0 + (r - \delta)T - \frac{1}{2}\Sigma^2 T, \Sigma\sqrt{T}\right), \tag{3.13}$$

with density function:

$$f_{S_T|S_0}(S) = \sum_{i=1}^{N} \frac{\lambda_i}{\sqrt{2\pi T} S \sigma_i} \exp\left\{ -\frac{\left(\ln \frac{S}{S_0} - (r - \delta - \frac{1}{2}\sigma_i^2)T \right)^2}{2\sigma_i^2 T} \right\}. \tag{3.14}$$

To price an European Call Option, we take the expected present value of its future payoff under the risk neutral measure:

$$\begin{aligned}
C_{MLN} &= E^Q[(e^{-rT}(S(T) - K)^+] \\
&= e^{-rT} E^Q[(\sum_{i=1}^{N} 1_{C=i} S_i(T) - K)^+] \\
&= e^{-rT} E^Q[E^Q[(\sum_{i=1}^{N} 1_{C=i} S_i(T) - K)^+ \mid C]] \\
&= e^{-rT} \sum_{i=1}^{N} E^Q[(S_i(T) - K)^+] Q(C = i) \\
&= \sum_{i=1}^{N} \lambda_i e^{-rT} E^Q[(S_i(T) - K)^+] \\
&= \sum_{i=1}^{N} \lambda_i C_{BS}^i,
\end{aligned} \tag{3.15}$$

where C_{MLN} denotes the Call option price under our MLN model and C_{BS}^i denotes the price corresponding to component process $S_i(t)$ under the Black-Scholes model. Here the advantage of our simple mixing processes (equation 3.3) becomes apparent as they are essentially the same Geometric Brownian Motion as the one used under the Black-Scholes framework (equation (2.1)) except for the parameters. This allows us to reach our final result in equation (3.15) by risk neutral pricing. For put options with maturity payoff $(K - S(T))^+$, only a trivial modification is required to obtain:

$$P_{MLN} = \sum_{i=1}^{N} \lambda_i P_{BS}^i, \tag{3.16}$$

The above derivation serves as the proof for the following key proposition.

Propositon 3.2.1: *Consider a European stock (either call or put) option under risk neutral pricing and the MLN model specified by equation (3.13). The stock price process $S(t)$ has mixing components $S_i(t)$ with corresponding weights λ_i and volatilities σ_i for $i \in \{1, 2, ...N\}$. The arbitrage free option price is equal to a linear combination of Black-Scholes option prices from the components weighed by the mixing weights.*

A more detailed proof using partial expectations is presented in Appendix B. This proposition also concludes this section on MLN model specifications. In summary, we are making the Black-Scholes assumption introduced in Chapter 2 for each component stock price process. The resultant option pricing formula is in the form of a linear combination of component option prices, which is quite intuitive. However, recall that the volatility is not in such a nice form (see equation (3.6) in Proposition 3.1). This is the reason that the MLN model produces desired volatility smiles. It is also interesting to see that to some extent, the component density function values act as weights in the contribution to total volatility by each component volatility. In the next section, we will look at the option Greeks under the MLN model and their implications for hedging.

3.2.2 Option Greeks and Hedging

This section is a direct extension from the previous one. Here we consider option Greeks used frequently for hedging purposes, which may be of particular interest to market makers and dealers. In risk management practices, an option portfolio is hedged through buying or selling other assets and derivatives, which often include the underlying stock and other options. Hedging is usually done dynamically so that the portfolio must be rebalanced periodically, which incurs considerable transaction costs. Here we treat these costs as externalities and only present the theoretical hedging formula under the Mixture Lognormal model specified in the previous section. The empirical effectiveness of the hedging technique is beyond our study.

We adopt the same option Greeks notation as commonly used under the Black-Scholes Framework and its extensions. The formulas are included in Appendix C.

1. Δ: the derivative of option price with respect to the underlying stock price ($\frac{\partial C}{\partial S}$ or $\frac{\partial P}{\partial S}$). It is positive for call options and negative for put options [2].

[2]To be precise, under the Black-Scholes framework, we have $\Delta_{call} \in (0, 1)$ and $\Delta_{put} \in (-1, 0)$

2. γ: the derivative of option with respect to the underlying stock price. Δ ($\frac{\partial^2 C}{\partial S^2}$ or $\frac{\partial^2 P}{\partial S^2}$). It is positive and the same for call and put options.

3. θ: the derivative of option price with respect to time to maturity ($\frac{\partial C}{\partial T}$ or $\frac{\partial P}{\partial T}$). As the option approaches maturity, its intrinsic value decreases, making this Greek often negative for both call and put options

4. ρ: the derivative of option price with respect to the continuous risk free rate($\frac{\partial C}{\partial r}$ or $\frac{\partial P}{\partial r}$). It is usually positive for call options and negative for put options.

5. ψ: the derivative of option price with respect to the continuous dividend rate ($\frac{\partial C}{\partial \delta}$ or $\frac{\partial P}{\partial \delta}$). It is usually negative for call options and positive for put options.

6. ν: the derivative of option price with respect to the volatility term. ($\frac{\partial C}{\partial \sigma}$ or $\frac{\partial P}{\partial \sigma}$). It is usually positive for both call and put options.

An obvious departure of the Greeks in our MLN model from those in the Black-Scholes model is ν. By definition, stock return volatility under the MLN model is directly governed by multiple component volatility parameters as shown in equation (3.6). This subtle point is not explored in many previous studies. Proposition 3.2.1 in the earlier section gives the pricing formula of a stock option price under the MLN model, which simply equals a linear combination of Black-Scholes prices from component stock price processes. Due to the linearity of differential operators, we claim that each option Greek is also in the form of a linear combination of Black-Scholes option Greeks from the component processes. However, ν is an exception to this rule as a single explicit volatility term does not appear in the option pricing formula. Therefore, it is necessary to define partial-ν terms denoted by ν^i_{MLN}.

Definition 3.2.2: *Consider a European stock (either call or put) option under risk neutral pricing and the MLN model specified by equation (3.13). The stock price process $S(t)$ has mixing components $S_i(t)$ with corresponding weights λ_i for $i \in \{1, 2, ...N\}$. The option Greek ν^i_{MLN} is the derivative of the option price with respect to volatility in component process i (e.g. $\frac{\partial C}{\partial \sigma_i}$ or $\frac{\partial P}{\partial \sigma_i}$).*

The formula for partial ν is easily derived:

$$\nu^i_{MLN} = \frac{\partial C}{\partial \sigma_i} = \frac{\partial \sum_{j=1}^{N} \lambda_j C^j_{BS}}{\partial \sigma_i} = \sum_{j=1}^{N} \lambda_j \frac{C^j_{BS}}{\sigma_i} = \lambda_i \nu^i_{BS}, \tag{3.17}$$

where ν^i_{BS} denotes the Black-Scholes option ν from component process i.

With this formula and the relationship described in equation (3.6) we are able to obtain a solution for the traditionally defined ν Greek under our MLN model by the chain rule of differentiation. However, it is numerically demanding and the component volatility terms still remain in the result, which is cumbersome for analysis. For a hedging purpose, it can be easily inferred that when all component process volatilities are hedged simultaneously, so is the overall volatility. Therefore, we consider portfolios that are partial-ν neutral to be volatility hedged, which we strive to achieve. For all other option Greeks, a natural conclusion can be drawn as follows.

Proposition 3.2.2: *Consider a European stock (either call or put) option under risk neutral pricing and the MLN model specified by equation (3.13). The stock price process $S(t)$ has mixing components $S_i(t)$ with corresponding weights λ_i for $i \in \{1, 2, ...N\}$. Any option Greek properly defined under the MLN model is equal to a linear combination of the corresponding Black-Scholes option Greeks from the components weighed by the mixing weights.*

For illustrative purpose, it is sufficient to present the derivation for Δ as given below.

$$\Delta_{MLN} = \frac{\partial C}{\partial S} = \frac{\partial}{\partial S} \sum_{i=1}^{N} \lambda_i C^i_{BS} = \sum_{i=1}^{N} \lambda_i \frac{\partial C^i_{BS}}{\partial S} = \sum_{i=1}^{N} \lambda_i \Delta^i_{BS}, \tag{3.18}$$

where Δ^i_{BS} denotes the Black-Scholes Δ from component process i.

So far we have presented the concepts of, and constructed the required results for, option Greek hedging under our MLN model specified in previous sections. Notice that the mixing weights λ_i, $i \in \{1, 2...N\}$, are treated as stable parameters recalibrated periodically and thus not a risk exposure in the dynamic hedging process. Intuitively, the weights as defined in Definition 3.2.1 are probabilities that each component process dominates and thus can be viewed as a periodic market element, lending justification to our approach. Here we provide an example of hedging. Notice that this is only a theoretical example where parameters are given information. In practice, all parameters need to be calibrated, which we will discuss in the next sections.

Example 3.2.2: delta-gamma-vega hedging

We hold a European call option of Microsoft stock with strike price \$29 *maturing in 3*

months. The Microsoft stock currently trades at \$30*/share. In annual terms, the continuously compounded risk free rate is* 3% *and the continuously compounded dividend rate is* 1%*. Assume that the MLN option pricing framework holds true in the market and we have confirmed the effectiveness of a 2 component process MLN model. Through calibration we determined mixing weights* $\lambda_1 = 0.25$ *and* $\lambda_2 = 0.75$ *as well as component volatilities* $\sigma_1 = 0.2$ *and* $\sigma_2 = 0.4$*. Next we construct a Delta-Gamma-Vega neutral portfolio that completely hedges our exposure using:*

1. *European call option on Microsoft stock with strike price* \$31 *maturing in 3 months*
2. *European call option on Microsoft stock with strike price* \$28 *maturing in 1 month*
3. *European put option on Microsoft stock with strike price* \$31 *maturing in 2 months*

The solution is presented below.

We denote the d_j quantity obtained from component process i by d_j^i, $j \in \{1, 2\}$ and for this case $i \in \{1, 2\}$. We also denote an Black-Scholes option Greek from component process i by adding a superscript to the corresponding Black-Scholes notation. Using the provided information, we apply equations (2.10) and (2.11) as well as the option Greek formula in Appendix C. The result is presented in Table 3.1 below.

Option	C($K = 29, T = \frac{3}{12}$)	C($K = 31, T = \frac{3}{12}$)	C($K = 28, T = \frac{1}{12}$)	P($K = 31, T = \frac{2}{12}$)
d_1^1	0.439016	−0.227898	1.252727	−0.319942
d_2^1	0.339016	−0.327898	1.194992	−0.401592
d_1^2	0.294508	−0.038949	0.669665	−0.098734
d_2^2	0.094508	−0.238949	0.554195	−0.262033
Δ_{BS}^1	0.668003	0.408839	0.894102	−0.624452
Δ_{BS}^2	0.614277	0.483256	0.747841	−0.538427
γ_{BS}^1	0.120462	0.129248	0.105006	0.154484
γ_{BS}^2	0.063510	0.066274	0.091955	0.080903
ν_{BS}^1	5.420805	5.816175	1.575087	4.634512
ν_{BS}^2	5.715857	5.964667	2.758665	4.854171

Table 3.1: Calculation for example 3.2.2 - component process Greeks

Now we apply Proposition 3.2.2 and equation (3.17) to find the Greeks under the MLN model. The option prices are calculated using Proposition 3.2.1 and the Black-Scholes option price formulas in Chapter 2. Again, for volatilities we are effectively hedging the

partial-ν in Definition 3.2.2. With given mixing weights, the result is summarized in Table 3.2 below.

option	C($K=29, T=\frac{3}{12}$)	C($K=31, T=\frac{3}{12}$)	C($K=28, T=\frac{3}{12}$)	P($K=31, T=\frac{2}{12}$)
Price	2.67	1.72	2.48	2.22
Δ_{MLN}	0.627709	0.464652	0.784406	-0.559933
γ_{MLN}	0.077748	0.082018	0.095218	0.099298
ν^1_{MLN}	1.355201	1.454044	0.393772	1.158628
ν^2_{MLN}	4.286893	4.473500	2.068999	3.640628

Table 3.2: Calculation for example 3.2.2 - option Greeks under the MLN model

This hedging problem is then transformed into solving a system of linear equations. The key is to hedge the γ and ν^i_{MLN} first to ensure the existence of a solution as any excess Δ can always be hedged using the underlying stock. Let w_1, w_2, and w_3 represent the number of each type of options to be purchased. We need to solve:

$$\begin{bmatrix} 0.082018 & 0.095218 & 0.099298 \\ 1.454044 & 0.393772 & 1.158628 \\ 4.473500 & 4.473500 & 3.640628 \end{bmatrix} \begin{bmatrix} w_1 \\ w_2 \\ w_3 \end{bmatrix} = \begin{bmatrix} -0.077748 \\ -1.355201 \\ -4.286893 \end{bmatrix},$$

where we obtain the result

$$\begin{bmatrix} w_1 \\ w_2 \\ w_3 \end{bmatrix} = \begin{bmatrix} -1.1396 \\ -0.1651 \\ 0.3166 \end{bmatrix}.$$

The net Δ exposure is:

$$\begin{bmatrix} 0.627709 & 0.464652 & 0.784406 & -0.559933 \end{bmatrix} \begin{bmatrix} 1 \\ -1.1396 \\ -0.1651 \\ 0.3166 \end{bmatrix} = -0.2086,$$

which we hedge by buying 0.2086 shares of Microsoft stock. The net cost of hedging is then:

$$\begin{bmatrix} 30 & 1.72 & 2.48 & 2.22 \end{bmatrix} \begin{bmatrix} 0.2086 \\ -1.1396 \\ -0.1651 \\ 0.3166 \end{bmatrix} = 4.59,$$

There are several intuitions we may obtain from this example. First of all, it is apparent that our result only occurs in a theoretical setting as the total cost of the hedging instruments exceeds the price of the hedged option. This phenomenon is rare in the Black-Schole framework, where the risk is captured by a single volatility term. It happens in our MLN model most likely due to "over-hedging", where we effectively hedge each component volatility fluctuation.

In addition, notice that the ranges of the Black-Scholes option Greeks also apply to the MLN Greeks. This result is not coincidence and can be proved without loss of generality using option Δ. As a direct result of Proposition 3.2.2 above, we have:

$$\sum_{i=1}^{N} \lambda_i \min\{\Delta_{BS}^i \mid i = 1, 2..N\} \leq \Delta_{MLN} \leq \sum_{i=1}^{N} \lambda_i \max\{\Delta_{BS}^i \mid i = 1, 2..N\},$$

which then gives:

$$0 \leq \Delta_{MLN} \leq 1$$

Lastly, we used the two-component MLN model in this example, which is numerically efficient. The two-component model is the simplest example of the MLN framework we have established to be capable of capturing volatility smiles in most situations. Not surprisingly, its simplicity leads to some additional desirable properties, which we will discuss in the next section.

3.2.3 Dynamics of the Two-component Mixture model

In this subsection, we reproduce the discussion in Neumann (2002)[35] and adapt it to the setting of this thesis by placing special emphasis on the ability of the model to generate the volatility smile phenomenon observed in the markets. When the MLN model assumes its simplest form, only two component price processes are involved, which we denote by two triplets: (S_1, μ_1, σ_1) and (S_2, μ_2, σ_2). In addition, we let λ denote the mixing weight for S_1 (traditionally denoted by λ_1). As a direct result, the mixing weight for S_2 equals $1 - \lambda$. Under the same time frame of interest $t \in [0, T]$ and probability space (Ω, F, P) as stated earlier, the diffusion processes are just an example of equation (3.3):

$$dS_1(t) = \mu_1 S_1(t)dt + \sigma_1 S_1(t)dZ(t),$$
$$dS_2(t) = \mu_2 S(t)dt + \sigma_2 S_2(t)dZ(t),$$

with common initial conditions:

$$S_1(0) = S_2(0) = S_0.$$

Moreover, the density function of the stock price $S(t)$ is an example of equation (3.11) and equation (3.14):

$$f^{mix}_{S_t|S_0}(s; \lambda, m_1, m_2, v_1, v_2) = \lambda f^{LN}(s; m_1, v_1) + (1-\lambda) f^{LN}(s; m_2, v_2), \tag{3.19}$$

where $f^{mix}_{S_t|S_0}$ denotes the density function of the stock price at time t conditioning on the current stock price and f^{LN} denotes the lognormal density function as the one used in Definition 3.2.1. As before, we use m_i and v_i to represent the mean and standard deviation parameters to avoid confusion.[3] Under the MLN model, Proposition 3.2.1 applies to give:

$$C_{MLN} = \lambda C^1_{BS} + (1-\lambda) C^2_{BS}, \tag{3.20}$$
$$P_{MLN} = \lambda P^1_{BS} + (1-\lambda) P^2_{BS}. \tag{3.21}$$

While the above contents has no additional derivation, the simplicity of the two-component mixture allows us to study the stock price directly, which would otherwise be clumsy for a greater number of components. First note that the expected value and variance of a lognormally distributed random variable S_T at time point $t \in [0, T]$ is given by:

$$E_t[S_T] = e^{m + \frac{1}{2}v^2}, \tag{3.22}$$
$$Var_t(S_T) = (e^{v^2} - 1)(e^{2m+v^2}), \tag{3.23}$$

where the subscript t indicates expected value is taken with the σ-algebra at time t. Now, let S^1_t and S^2_t be the time t discounted expected values of the component stock prices. That is to say:

$$S^1_t = e^{-r(T-t)} E_t[S_1(T)], \tag{3.24}$$
$$S^2_t = e^{-r(T-t)} E_t[S_2(T)]. \tag{3.25}$$

[3] As we essentially assume the same Black-Scholes framework for each component process, we have $m_i = \ln S_0 + (\mu_i - \delta - \frac{1}{2}\sigma_i^2)(T-t)$ under (Ω, F, P) or $m_i = \ln S_0 + (r - \delta - \frac{1}{2}\sigma_i^2)(T-t)$ under the risk neutral measure (Ω, F, Q), and $v_i = \sigma_i \sqrt{T-t}$ for both cases, $i \in \{1, 2\}$.

These two variables are completely determined by the martingale restriction of the underlying time-t stock price S_t:

$$\begin{aligned} S_t =& e^{-r(T-t)} E_t[S(T)] \\ &= e^{-r(T-t)} E_t[E_t[S(T) \mid C]] \\ &= S_t^1 P(C=1) + S_t^2 P(C=2) \\ &= \lambda S_t^1 + (1-\lambda) S_t^2. \end{aligned} \tag{3.26}$$

As a result, the observed stock price S_t must satisfy the following equation:

$$S_t^2 = \frac{S_t - \lambda S_t^1}{1-\lambda}. \tag{3.27}$$

It is easy to see that the stock price is actually a linear interpolation of the expected component prices. Let us assume that $S_t^1 \leq S_t^2$, which is equivalent to saying that $S_t^1 \leq S_t$. Then λ can be viewed as the probability that a low asset price market dominates. S_t^1 therefore follows this interpretation and is referred to as the downside component in this thesis. This property enables the model to capture the phenomenon of crash-o-phobia, which is the strong negative skews in the implied stock return distribution. The cause of the crash-o-phobia extends beyond the general market's fear of crash.[4] The level of crash-o-phobia effect depends on the parameters S_t^1 and λ, where a low level of S_t^1 implies potential significant drop of the underlying stock price perceived by the market. The magnitudes of component volatilities σ_i are also proportional to the stock price levels in each market condition represented by the components.

Nevertheless, option prices follow the path given by the general diffusion $S(t)$ and not only on the first(downside) component $S_1(t)$. Consequently, both component volatilities enter the option pricing formula under the MLN model. As mentioned earlier when discussing option Greeks under the MLN model in Section 3.2.3, there is no explicit single measure of volatility in the MLN option pricing formula. However, an appropriate risk measure, namely the variance of the mixture distribution, can be derived for this two-mixture case as its simplicity encourages us to neglect equation (3.6) and work with the moments directly. The result can be summarized in the following proposition, where the detailed proof of this proposition is in included in Appendix D.

[4] In fact, one economic rationale is that put options have been widely used as hedging instruments for stocks to protect against significant losses. This generally adopted strategy bid up prices of put options relative to call options and create a negative skew in the implied stock returns.

Proposition 3.2.3: *Consider a stock price under the MLN framework specified in Section 3.1-3.2.1 with two component processes (S_1, μ_1, σ_1) and (S_2, μ_2, σ_2) with mixing weights λ and $1-\lambda$. Then the variance of the terminal stock price distribution evaluated at time $t \in [0, T]$ can be decomposed as follows:*

$$\begin{aligned} Var_t(S(T)) =& \lambda Var_t(S_1(T)) + (1-\lambda) Var_t(S_2(T)) \\ &+ \lambda(1-\lambda)(E_t[S_1(T)] - E_t[S_2(T)])^2. \end{aligned}$$

Obviously, the variance of the mixture distribution for the time T stock price consists of the weighted variances of the components and the distance between the expectations of the components. Notice that this decomposition does not yield such a nice form when the number of component price processes increases.

With this information about the composition of the terminal stock price distribution under mixture diffusion, it is possible to calculate the contribution of the first component to the total variance of the mixture distribution. Therefore, we define the share of downside risk(SDR).

Definition 3.2.3: *Under the two-factor MLN model specified in this section, the share of downside risk (SDR) is a measure of the contribution to the total variance of the mixture stock price distribution by the first component distribution corresponding to low price market condition:*

$$SDR_t = \frac{Var_t(S(T)) - (1-\lambda)(Var_t(S_2(T)))}{Var_t(S(T))}.$$

SDR is a good indicator for the influence of the downside component to the pricing of options. In addition, this calibrated risk measure resonates in definition with the interpretation we provided for the component price variables in this section. Notice that it can also be easily modified to accommodate other risk management frameworks as a market statistic implied by derivatives.

The approach of a two-component mixture presented in this section is straightforward and utilizes our MLN framework in its simplest form. Nevertheless, this approach still incorporates the possibility of future extreme underlying price movements. The Law of Parsimony also recommends that we start from this two-factor approach as more complex

models must display a significant level of improved fits for them to be selected. The empirical analysis in the next section will assess whether two mixture components are sufficient for the pricing of S&P 500 index options.

3.3 Calibration Techniques

So far we have specified and discussed the MLN option pricing model. The framework stems from a mixture of diffusion processes adopting lognormal component density functions. This lognormal nature simplifies the derivation process and leads us to a closed form option pricing formula as described in Proposition 3.2.1. We have also studied the two-component mixture as the simplest example under the MLN framework. A comprehensive study of the three-component MLN model and its pricing performance on an individual stock is done by Brigo et.al. (2002)[4], where the capability of such a model in producing volatility smiles is demonstrated in a hypothetical setting. We now test the effectiveness of the two-component model on index options using S&P 500 option price data. In particular, we examine its pricing accuracy as well as capability in generating volatility smiles, which is absent in the traditional Black-Scholes context. As published literature reveals little about the calibration of mixture models, for simplicity, we propose and implement a calibration technique using least square error

3.3.1 Data Structure and Calibration Methodology

Due to various limitations, historical high frequency tick-by-tick option quotes are not available to our research. Therefore we adopt an alternative approach of manually collecting and organizing end of day option chain information published by the Chicago Board of Trade. For a systemic investigation, we vary the underlying index price by aggregating the information over several trading days.

The raw information collected consists of all daily closing quotes (e.g. bid price, ask price, volumes, and interests) for S&P500 index option traded on Chicago Board of Exchange(CBOE) for 7 non-consecutive trading days from June 19, 2012 to June 29, 2012. To create our sample, we first eliminate non-European style options (e.g. binary options, which is studied later in the next chapter). Then, as a noise reduction effort, we keep only the traditional European option quoted as "SPX" on CBOE and exclude both the weekly (SPXW) and quarterly (SPXQ) options though they are extremely similar to the SPX option. We do not exclude non-actively traded options as their bid-ask prices still carry

fair information of the market. For a calibration purpose, we use the midpoint between bid and ask as an estimate of the true value of the option. This gives us a 7-day time series panel of call and put option prices. The prices are then matched with the daily closing S&P 500 index levels for the corresponding day to create our final sample, where each data row is a combination of option price (C for call and P for put), underlying index price S, strike price K, and time to maturity T. As expected, no two rows are identical.

The MLN model parameters for each day is calibrated separately from others. This yields a 7-day time series of mixture weights λ_i and component volatilities σ_i, $i \in \{1...N\}$. The main advantage of this approach is that it obeys the definition of local volatility and admits the fact that volatility itself is non-constant and time-varying. It also minimizes the effects of the discontinuity in data collection. Notice that the time window can be extended to obtain more observations in practice.

Several advantages arise by using S&P500 index option data as our sample. First of all, it is consistent with the approaches taken by most previous researches on the Black-Scholes framework and thus forms a good comparative basis. Secondly, it avoids company-specific factors such as firm dependent skewness and kurtosis shapes mentioned in Chapter 1. Lastly, the underlying index pays no dividend. This greatly simplifies our numerical procedure as the calibration of a stable continuously compounded dividend rate is expected to introduce more uncertainty to the model.

On the other hand, significant challenges are brought by this dataset. First of all, as S&P500 option is exchange-traded, its bid and ask prices change in fixed minimum steps. This conceals information about the exact market price. In addition, the midpoint of the bid-ask pair is used as the best approximation of market option price. The quality of this approximation is likely to become worse when the bid-ask spread is large, which results in unreasonable prices in the data[5]. We treat those cases as noises and remove them from the sample set. This is why the sizes of the final sample tend to differ for each day. However, we state as a qualification that both factors will remain inevitable as a source of bias.

The risk free interest rate r used for calculating theoretical option prices can be found through several methods. For a genuinely noise-free sample, it is best estimated by working with the put-call parity condition as suggested by Shimko (1993)[40] using the two pairs of put and call options closest to at the money with identical maturity. Theoretically, a

[5]This includes, for instance, cases where a call option with a higher strike costs less than an otherwise identical option with a lower strike

single pair of at the money call and put options with identical terms is sufficient for the estimation of a risk free rate with minimal noise. However, as options are standardized contracts in the exchange, exactly at-the-money options are rare. On the contrary, for a sample requiring a noise reduction measure, subjective input from economics information performs better as the sample-estimated rate is vulnerable to bias source[6]. To be conservative, we choose the latter approach in the implementation stage. Notice that, to be consistent with the traditions in most previous work on the Black-Scholes model, we ignore the term structure of interest rates and assume its differential effects offset each other overall.

Calibration of the MLN model may also be performed through several different numerical procedures. Heuristically, stock return parameters such as local volatilities are calculated through conditional maximum likelihood estimations (MLE). The rationale is based on the assumption of the lognormal stock price distribution in the Black-Scholes framework. It takes advantage of the unique MLE features of lognormal random variables, where consecutive log returns are independent normal variables whose mean and variances have estimators with well established statistical properties. However, this advantage is lost under our MLN model specified in Sections 3.1 and 3.2. The reason for this is that taking the logarithm of a mixture lognormal variable does not yield a corresponding mixture normal variable[7]. As a result, the conditional MLE technique requires us to derive maximum likelihood estimators from the mixture lognormal density function (equation (3.14)) directly, where a system of equations representing the first-order conditions does not have a nice closed form expression. The adoption of likelihood based technique will thus result in intractable numerical procedures for our MLN model.

For this reason, we propose an alternative calibration methodology using the principle of the least sum of square error. The data must be organized into the sample format in our case, where each data row is a unique combination of market option price with the corresponding underlying asset price, strike price, and time to maturity. For illustrative purpose we focus on call option only. Let n denote the sample size for each day. Let $c_j, j \in \{1..n\}\}$ be the observed option prices with corresponding theoretical price C_{MLNj} under our MLN framework. The calibration of the model parameters λ_i and σ_i, $i \in 1..N$,

[6]The vulnerability may be exemplified by negative calibrated risk free rates from near-maturity options

[7]In fact, to obtain such a result, the consecutive stock price ratios must be modelled by an exponential of a mixture normal variable, which is similar to the Regime Switching Model[17] that will be briefly discussed later in comparison with our MLN model.

is a process equivalent to solving the following optimization problem:

$$\begin{aligned} \underset{\lambda_i,\sigma_i}{\text{minimize}} \quad & \sum_{j=1}^{N}(C_{MLNj} - c_j)^2 \\ \text{subject to} \quad & \sum_{i=1}^{N}\lambda_i = 1, \\ & \sigma_i \geq 0, i \in \{1, ...N\} \\ & \lambda_i \geq 0, i \in \{1, ...N\} \end{aligned}$$

The complexity of the objective function renders standard algorithms such as the simplex method inefficient. Therefore, parameter estimates are calculated for each option series by performing a grid pattern search with non-linear regressions on observed and theoretical option prices. We implement this process using Matlab. Apparently, for the special case of only one mixture component we obtain the conventional lognormal distribution. As suggested previously, we will fit the two-component mixture model and examine its performance in comparison to the Black-Scholes model.

The unique features of the two-component MLN model introduced in Section 3.2.3 allows us to perform additional analysis beyond the testing of pricing accuracy of a general MLN model. It also affords an interpretation of the model involving downside risk. To measure the impact and/or improvements of introducing a downside risk, we may look at the evolution of the expected discounted downside component S_t^1 in equation (3.24) and the Share of Downside Risk (SDR) introduced by Definition 3.2.3, which are both post-calibration analysis.

From the relevant formulas, we see that both measures require a good fit of S_t^1 value. Ideally, the quantities S_t^1 and S_t^2 are best estimated through an additional round of calibration using the intra-day high-frequency option and stock price quotes. However, such data is costly and may adversely affect the numerical efficiency. Therefore, we propose an alternative approach that calculates S_t^1 and S_t^2 value from the MLN model parameters. As we ignore transaction costs in this implementation, the martingale restriction in equation 3.26 can be imposed. However, equation (3.26) alone gives infinitely many solutions. Intuitively, it is desirable to maximize the differential component impacts from S_t^1 and S_t^2 to the overall discounted expected stock price. We measure this "impact" by the Contribution to Martingale Expectation(CME) under the MLN model, which is defined below.

Definition 3.3.1: *Under the risk neutral pricing and the MLN model specified in Chapter 3, the stock price process $S(t)$ has mixing components $S_i(t)$ with corresponding weights λ_i and volatilities σ_i for $i \in \{1, 2, ...N\}$. The Contribution to Martingale Expectation (CME) for component S_i measures the percentage of the true time-t stock price, S_t, attributed to the time-t discounted expectation from process S_i under the martingale restriction:*

$$CME_t^i = \frac{\lambda_i S_t^i}{S_t},$$

where, for the two-component case (i.e. $N = 2$) in Section 3.2.3, S_t^i is given by equation (3.24) and equation (3.25).

Notice that, by definition, we have $CME \in (0, 1)$, which guarantees the existence of an entropy H_t^i. In interpreting the model, each component corresponds to a market state. Thus, it is desirable to maximize the divergence in CME between components. We are therefore encouraged to set the S_t^1 and S_t^2 values, within their feasible regions, to the ones that maximize the entropy of the CME space. For the two-component model, this is equivalent to solving the following problem, where we replaced S_t^2 by its solution to equation (3.26) in terms of S_t^1:

$$\begin{aligned} \underset{S_t^1}{\text{maximize}} \quad & H_t = -\lambda S_t^1 ln(\lambda S_t^1) - (S_t - \lambda S_t^1) ln(S_t - \lambda S_t^1) \\ \text{subject to} \quad & S_t^i > 0, i \in \{1, 2\} \end{aligned}$$

This one-dimensional optimization problem has a continuous objective function within the defined domain and can be easily solved by working with its respective first and second order conditions. The derivations are provided in Appendix F. We obtain the following result:

$$\begin{aligned} \hat{S_t^1} &= \frac{S_t}{2\lambda}, \\ \hat{S_t^2} &= \frac{S_t}{2(1-\lambda)}, \end{aligned}$$

The optimal CME values associated with the above critical S_t^i values are 0.5 for both components. Apparently, the construct condition $S_t^1 \leq S_t$ is satisfied if and only if $\lambda > 0.5$. Therefore, this approach fully utilizes the market information and captures interactions

between the weight parameters and the component processes under the martingale restriction. It also allows us to examine the validity and significance of the downside component. If the condition is satisfied in all (or most) of the sample days, we can conclude the presence of strong empirical evidence in support of our model.

The rest of the analysis is straight-forward. To calculate the associated variance terms, we apply equation 3.23 to obtain:

$$Var_t(S_i(T)) = (S_t^i)^2 e^{2(r-\delta)(T-t)}(e^{\sigma_i^2(T-t)} - 1), \forall i \in \{1, 2\}. \tag{3.28}$$

As a consequence, the variance of the stock price at maturity can be calculated by Proposition 3.2.3 as:

$$\begin{aligned} Var_t(S(T)) =& \lambda(S_t^1)^2 e^{2(r-\delta)(T-t)}(e^{\sigma_1^2(T-t)} - 1) \\ &+ (1-\lambda)(S_t^2)^2 e^{2(r-\delta)(T-t)}(e^{\sigma_2^2(T-t)} - 1) \\ &+ \lambda(1-\lambda)(S_t^1 - S_t^2)^2 e^{2(r-\delta)(T-t)}. \end{aligned} \tag{3.29}$$

The time series of SRD can be then easily calculated by Definition 3.2.3 through a simple substitution of relevant quantities.

In summary, we will use the two-component MLN model for its ease of interpretation and implementation for the empirical example in the next section. The effect of downside risk is checked for its significance and impacts on index option prices. We also compare the in-sample results to those produced by the Black-Scholes model to see if any improvement exists for the MLN framework in pricing stable period index options. Most importantly, we verify that our MLN produces the desired level of implied volatility smile.

3.3.2 Empirical Results and Analysis

We present the empirical results of this section. As mentioned previously, we focus our analysis on call options only. The final sample of Call option quotes used for calibration is summarized in Table 3.3 below, where n denotes the sample size, S denotes the closing S&P500 quotes, and C denotes the call option price used for calibration. T and K respectively denote the time to maturity (years) and strike price (U.S. dollars) as usual. Notice that the moneyness η is defined differently from before.

Definition 3.3.2: *Consider a European Call option with market price C and strike price K. The moneyness η of this option is the percentage difference between the spot underlying stock price S and the strike price relative to the strike price:*

$$\eta = (S - K)/K$$

We will follow this definition from now on unless otherwise specified.

		19-Jun	21-Jun	22-Jun	25-Jun	26-Jun	28-Jun	29-Jun
n		767	759	764	759	763	761	763
S		1357.98	1325.51	1335.02	1313.72	1319.99	1329.04	1362.16
C	Max	1248.90	1216.81	1223.90	1205.05	1214.15	1221.05	1255.30
	Min	0.05	0.05	0.05	0.05	0.05	0.04	0.075
	Mean	300.34	282.32	288.17	278.47	282.30	287.27	308.08
	Sdev.	311.75	303.47	307.1013	301.8303	304.2660	306.4119	315.4625
	Skew.	1.0963	1.1447	1.1078	1.1336	1.1237	1.1083	1.0527
	Kurt.	3.3272	3.4300	3.3192	3.3784	3.3562	3.3213	3.2053
T	Max	2.5041	2.4986	2.4959	2.4877	2.4849	2.4795	2.4767
	Min	0.0877	0.0822	0.0795	0.0712	0.0685	0.0630	0.0602
	Mean	0.7125	0.7110	0.7090	0.7026	0.6979	0.6934	0.6871
	Median	0.4137	0.4082	0.4055	0.3973	0.3945	0.3890	0.3863
	Sdev.	0.7474	0.7488	0.7464	0.7481	0.7468	0.7475	0.7481
K	Max	3000	3000	3000	3000	3000	3000	3000
	Min	100	100	100	100	100	100	100
	Mean	1137.10	1131.11	1129.50	1124.64	1127.63	1126.22	1124.16
	Median	1190	1180	1180	1175	1175	1175	1175
	Sdev.	424.33	421.56	425.16	422.83	423.85	423.30	418.4085
η	Max	12.5800	12.2551	12.3502	12.1372	12.1999	12.2904	12.6216
	Min	-0.5897	-0.5582	-0.5550	-0.5621	-0.5600	-0.5570	-0.5459
	Mean	0.5897	0.5597	0.5745	0.5552	0.5585	0.5712	0.6099
	Median	0.1412	0.1233	0.1314	0.1181	0.1234	0.1311	0.1593
	Sdev.	1.5819	1.5502	1.5577	1.5364	1.5407	1.5528	1.5891

Table 3.3: Summary of call option data used for calibration

Notice that for all 7 days, the mean and median moneyness values are not far from zero as we expect, indicating that the sample is reasonable in spite of the defects and data noises

mentioned in the previous section. The time to maturity ranges from 0.060274(22 days) to 2.50411(914 days) and the strike price ranges from 100 to 3000. These large ranges facilitates our analysis of volatility smiles.

To calibrate the model parameters, we subjectively introduce a risk-free rate of 2%, which is consistent with the economic conditions for the period of interest. Using the proposed calibration methodologies in the previous section, the following parameter estimates are obtained for each of the seven days:

	19-Jun	21-Jun	22-Jun	25-Jun	26-Jun	28-Jun	29-Jun	Mean	Sdev.
λ	0.6399	0.6245	0.5997	0.5874	0.7219	0.6625	0.7036	0.6485	0.0506
σ	0.1464	0.1534	0.1448	0.1526	0.1523	0.1476	0.1386	0.1480	0.0053
σ_1	0.1461	0.1530	0.1444	0.1521	0.1518	0.1472	0.1382	0.1476	0.0053
σ_2	0.1472	0.1545	0.1452	0.1535	0.1535	0.1484	0.1396	0.1488	0.0054
S_t	1357.98	1325.51	1335.02	1313.72	1319.99	1329.04	1362.16	1334.77	18.5702
S_t^1	1061.10	1061.24	1113.01	1118.25	914.22	1003.09	967.97	1034.12	75.8065
S_t^2	1885.52	1765.05	1667.66	1592.01	2373.43	1968.81	2297.94	1935.77	301.53

Table 3.4: Fitted parameters for the MLN model and Black-Scholes model

We see that the volatility under Black-Scholes framework and the component volatilities under the MLN framework all fall within the 13%-15% range. In addition, for each day, the two-component volatilities are not substantially different. This is consistent with the general economic market condition for the period of our study, during which both the index level and interest rate are fairly stable with little sign of extreme conditions. Volatility stability and absence of stylized volatility patterns also correspond to the observation that estimated component volatilities display immaterial difference. A more pronounced difference can be expected for options of individual stocks, where company-specific risk has a much higher potential in driving the price further in both directions. Nevertheless, the fact that $\sigma_1 < \sigma < \sigma_2$ is consistent with our expectation, leading to a higher range of distribution component corresponding to high and low underlying prices when compared to a single lognormal distribution. In addition, the condition $S_t^1 < S_t < S_t^2$ is well satisfied for all 7 sample days. Simple calculation reveals that on average, S_t^1 is 22.51% lower than S_t while S_t^2 is 45.03% higher than S_t for our sample. As discussed in the previous chapter, the fitted component expectations are determined by the interactive effect of the probabilities and price expectations for high and low market conditions implied in the market data. Such an observation can therefore be taken as reasonable evidence of the existence of downside risk and crash-o-phobia. These risks are captured by the MLN model but not the

Black-Scholes model where we have a single component ($N = 1$) and $S = S^2$. A summary on the evolution of the downside risk for selected maturities (in days) is presented in Table 3.5 below. Notice that to form a comparable basis, we fix the time to maturities for all sample days, which, thus, may not correspond to existing options traded.

	$T-t$	19-Jun	21-Jun	22-Jun	25-Jun	26-Jun	28-Jun	29-Jun
	30	1985	2176	2133	2389	1589	1800	1477
$Var(S_1(T))$	178	12021	13182	12917	14472	9626	10905	8942
	365	25298	27756	27180	30470	20267	22952	18807
	729	53149	58372	57088	64073	42615	48228	39467
	30	6355	6138	4840	4930	10958	7045	8493
$Var(S_2(T))$	178	38493	37192	29314	29874	66398	42672	51418
	365	81016	78323	61687	62907	139816	89819	108158
	729	170234	164759	129581	132309	294070	188765	227016
	29	160691	120204	77307	58015	433060	212791	373643
$Var(S(T))$	178	181255	140644	94781	76297	461292	234269	397669
	365	208370	167642	117853	100472	498414	262566	429215
	729	264954	224138	166094	151150	575548	321541	494605
	29	0.9858	0.9808	0.9749	0.9649	0.9930	0.9888	0.9933
SDR	178	0.8187	0.7761	0.7355	0.6682	0.8780	0.8447	0.8886
	365	0.6680	0.6043	0.5522	0.4691	0.7620	0.7083	0.7828
	729	0.4521	0.3785	0.3331	0.2590	0.5675	0.5000	0.6051

Table 3.5: Estimated crash-o-phobia parameters of selected times to maturity

From the table, no clear time series trend is observed for the Share of Downside Risk (SDR) measure across the sample days. However, as the estimated component volatilities do not differ much, the SDR decreases rapidly for larger times to maturities in this case. In spite of this, the prominence of the downside component S_1 is still apparent for our dataset as the SDR take material values without showing diminishing pattern.

The empirical results so far confirms the significance of the additional component capturing downside risk and crash-o-phobia effects in our two-component MLN model. These findings are crucial as the implied volatility can be more readily replicated by the MLN framework when mixture models are recommended by market data. Now we compare the pricing accuracies of the two models.

The resultant prices from the two models are presented in Table 3.6 below for each sample day, where MSE, MAE, MPE stand for "mean square error, "mean absolute error", and "mean percentage error" respectively.

		19-Jun	21-Jun	22-Jun	25-Jun	26-Jun	28-Jun	29-Jun
MLN Prices	$\mu(C)$	309.3458	290.4542	298.2489	286.7256	289.3501	295.5416	317.1228
	$\sigma(C)$	323.5973	315.2607	319.6783	313.6970	315.2579	318.1074	326.9159
	MSE	375.4110	356.0509	412.0614	360.8936	330.7851	366.5772	387.0121
	MAE	10.6560	10.1759	11.3880	10.1848	9.3159	10.0881	10.3425
	MPE	21.18%	18.26%	16.29%	13.84%	13.59%	13.60%	13.74%
BS Prices	$\mu(C)$	309.3295	290.4322	298.2565	286.7113	289.3576	295.5375	317.1199
	$\sigma(C)$	323.6077	315.2739	319.6734	313.7057	315.2534	318.1099	326.9179
	MSE	375.4096	356.0529	412.0609	360.8918	330.8829	366.5862	387.0106
	MAE	10.6572	10.1771	11.3876	10.1858	9.3156	10.0883	10.3428
	MPE	21.02%	18.04%	16.36%	13.71%	13.65%	13.56%	13.71%

Table 3.6: Performance of fitted MLN and Black-Scholes models for European call

From statistics, we observe no clear improvement in prediction accuracy for the two-component MLN model over the traditional Black-Scholes model. As mentioned previously, the result may be heavily biased by data quality emanated directly from our choice of period under study. Similar result is shown by Figure 3.1 below, which is created from the aggregate data.

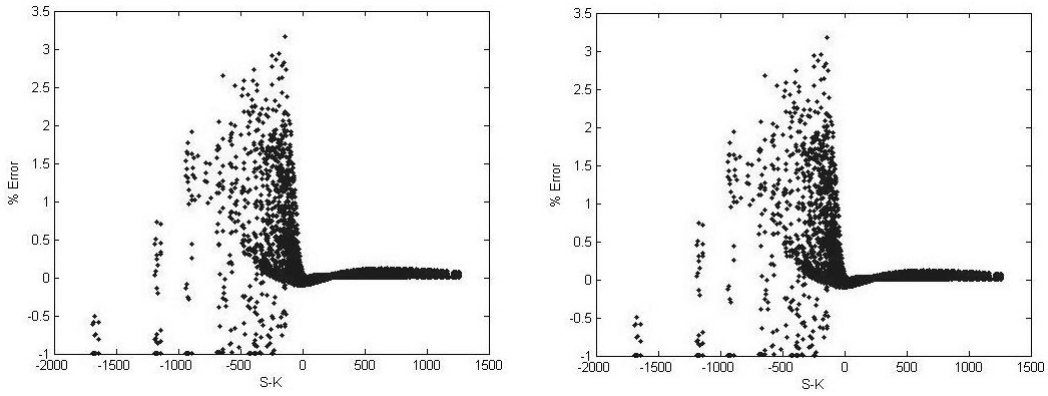

(a) Black-Scholes (b) MLN

Figure 3.1: Results for call option pricing, percentage error vs. spot-strike difference

The two charts plot the percentage pricing error versus the spot-strike difference calculated as $S - K$ from both models. It is observed that pricing errors display almost identical patterns. The well-known practical feature of the Black-Scholes model remains, where in-the-money call options are priced at much better accuracy than the out-of-the-money ones.

In summary, we see that for S&P500 index options, the two-component MLN model does not introduce material pricing improvements compared to Black-Schole model. At first, this seems to be contradicting the established theories as well as empirical findings in some studies. However, such observations can be well explained by the nature of our index option. As previously mentioned, S&P500 index has displayed very high stability and low volatility during the sample period. Compared to individual stocks, it has much less stylized fact in returns and volatilities. As a result, the two-component volatilities are close to each other as well as to the Black-Scholes volatility, obscuring the theoretical pricing improvements that are discovered for individual stock options. Therefore, all comparative analysis we generated in this section is particular to this index option, which still leads to valuation conclusions that constitutes our contribution to this topic of MLN models. Overall, we may state that compared to the traditional Black-Scholes model, the two-component mixture model does capture statistically significant downside risk underlying the S&P500 index but does not yield improved pricing accuracy for options due to a relatively tranquil market for the period under study.

To test if the two-component mixture generates desired volatility smiles, we switch to a semi-hypothetical setting as proposed by Brigo (2002)[4]. The theoretical capability of general MLN models in spanning maximal skewness and kurtosis domains is proved by Brigo (2002), who also illustrated the performance of three-component MLN model in generating volatility smiles. We take exactly the same approach to see if two-component model yield satisfactory smile-generating performance. To do so, we modify the calibrated parameters as the true results include extremely similar components that distort the performance. We randomly choose June 19, 2012 for demonstration and adopt new MLN parameter estimates: $\lambda = 0.65$, $\sigma_1 = 0.15$, $\sigma_2 = 0.45$. Notice the weight parameter is not varied much and where we widen the component volatility gap to create a semi-hypothetical setting, which can be well expected for high-volatility periods. We randomly select the call option maturing in 32 days ($T - t = 0.087671$) with strike prices ranging from $K = 800$ to $K = 1600$. The corresponding implied volatility is graphed below in Figure 3.2, where the horizontal axis represents the strike price.

The volatility figure exhibited a well-shaped smile, indicating that the two-component mix-

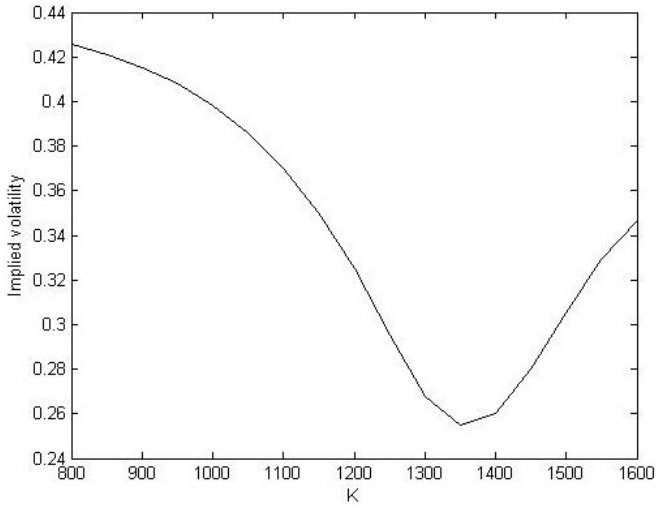

Figure 3.2: Implied volatility under MLN for call option maturing in 32 days

ture is sufficient for capturing volatility skews of S&P500 index options when component parameters are distinctive. To complete the analysis, we compare it with the market implied volatility as well as the Black-Scholes volatility estimate. Apparently, as we used hypothetical parameters in the MLN model for this purpose, the two volatility smiles are not expected to match in general magnitude. More specifically, the implied volatilities produced by our MLN model should be much greater than the market ones as we assumed high component volatilities. However, the overall shapes should be similar. The comparative result is presented in Figure 3.3 below.

From the graph, it is obvious that the result is expected. The implied volatility smile from our MLN model lies above the one from the market data at even distance, while the shapes of two are extremely similar. Notice that due to data quality problem discussed in the previous section and feasible region discontinuity embedded in the grid search algorithm, the market volatility smile contains noise points, though its overall shape still represents a typical volatility smile. The Black-Scholes volatility displays a flat line and is invariant to strike prices, which is a trivial result. Furthermore, observe that the MLN implied volatility is a little to the right of the market implied volatility. This can be corrected by introducing additional scale and shape parameters into the MLN model. Such complex models are closely studied in Brigo (2002) [4] and we do not discuss about this issue further here. A firm conclusion we can draw is that the two-component MLN model

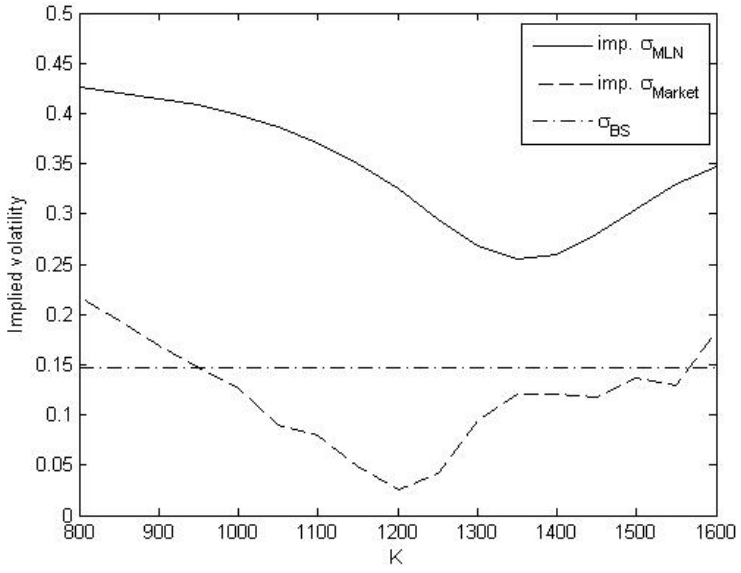

Figure 3.3: Comparative result of implied volatility smiles

does produce desired volatility smile shapes.

To justify our previous claim that similarity in component volatilities reduces the improvements of the MLN model over the Black-Schole model, we examine the effect on implied volatility smiles from varying the difference between component volatilities while keeping the mean unchanged. We add to our current case scenarios where i. $\sigma_1 = 0.2$ and $\sigma_2 = 0.4$, ii. $\sigma_1 = 0.25$ and $\sigma_2 = 0.35$, and iii. $\sigma_1 = 0.1$ and $\sigma_2 = 0.5$. The resultant smile is presented in Figure 3.4 below.

It is apparent that as the difference in the magnitude of component volatilities decreases, the implied volatility smile becomes flatter. As such trend propagates, extremely close component volatilities as in our case of S&P500 index option in tranquil period do not result in an observable smile. In fact, the pattern of the resulting implied volatility in this case resembles that of the Black-Scholes volatility for all strike-maturity combinations. This is consistent with our previous conclusion about pricing precisions.

In summary, we have studied the dynamics of mixture diffusion processes for stock price

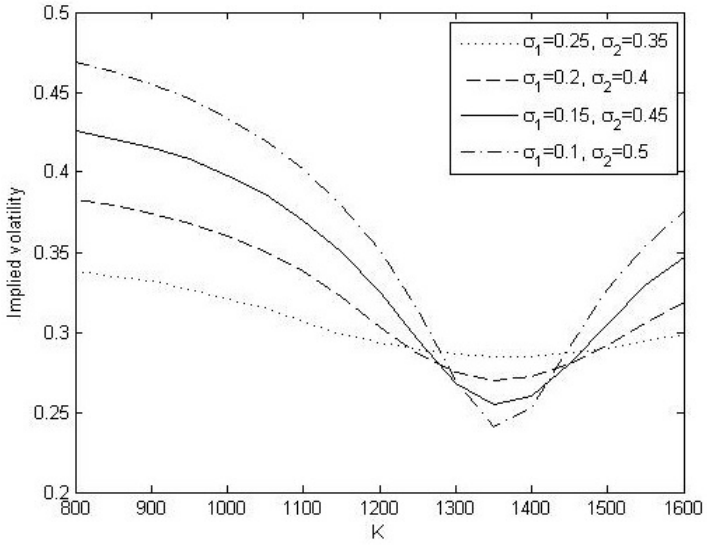

Figure 3.4: Implied volatility smiles under varying MLN volatility combinations

and specified the general Mixture Lognormal model (MLN) for European stock option pricing. We then focused on the two-component mixture as the simplest example of our MLN model with implementation for index option pricing during stable, low volatility periods. We confirm the existence of downside risk, which is not captured by the traditional Black-Scholes model. We found no clear improvement in S&P500 index option pricing by using the two-component MLN model under prolonged stable market conditions, suggesting that, in such an environment, the Black-Scholes model is sufficient for European option pricing purposes. Nevertheless, even the simplest two-component MLN model is shown to be capable of producing desired implied volatility smiles as illustrated under a semi-hypothetical setting. This is a unique feature we should exploit in future MLN model applications, particularly under periods of high volatilities and pronounced stylized returns.

3.4 Interpretation of the Mixture Model

The effectiveness of the MLN model in capturing implied volatility smiles was examined in the previous section. While we briefly interpreted the model in Section 3.2.3 under the two-component case, it can be extended to obtain an interpretation for the complete

MLN model that helps explain its advantages over the traditional Black-Scholes framework.

From a mathematical viewpoint, we look at our MLN model fully specified in Chapter 3.1 and 3.2.1. It is easy to see that the mixture is obtained by super-imposition of the components (S_i, μ_i, σ_i) with respect to the mixing weights λ_i, $i \in \{1...N\}$. The weights λ_i represent the probability mass function of the underlying state variable C choosing the diffusion process and can thus be viewed as a joint probability distribution of the drift and volatility parameters (μ_i, σ_i). Consequently, the assumption of a mixture of distributions in our MLN model leads to a specification with randomly changing parameters. This extra randomness captured by the MLN model is the main reason that the MLN model improves over the traditional Black-Scholes framework. While in the two factor model we treated the components as representatives of low price and high price markets, maximal complexity is obtained in the N component case. The state variable to some extent represents the aggregate effects of economic factors (e.g. low interest rate plus low inflation rate) as continuous scenarios, which we implicitly discretized by restricting the outcome to N cases. Apparently, for the two-component mixture, the aggregate effect is either a downside market or the reverse, a binary variable as shown in our model in Section 3.2.3.

From the viewpoint of economic theory, we obtain a similar interpretation, which is first pointed out by Neumann (2002)[35]. That is, Harris (1987)[18] argued that in a model where a number of agents trade in response to new information, the component variables can be perceived as random results of the major information events each day directed by the market state. Ignoring the evolution of such events and the triggered supply-demand shifts, our MLN model can be compared to models with stochastic volatility processes. Merton (1976)[34], for instance, assumes that the stock price experiences random jumps that can be captured by a jump-diffusion model. Other authors, such as Hull/White (1987)[23], provide a separate diffusion process for volatility as mentioned previously in Chapter 2.2. A theoretical study of the lognormal mixture models as approximations to the jump diffusion process and the stochastic volatility model is studied by Leisen (2004)[29]. Though significant complexities are required to be added to the simple lognormal mixture, the convergence in distribution result implies that a mixture process potentially combines advantages of both models (by Merton[34], and Hull and White[23]).

Another interesting fact worth mentioning at this stage is the relationship between the MLN model we specified and the Regime Switching Model for long term stock returns studied by Hardy (2001)[17]. Although both frameworks assume mixture distributions of stock returns, the nature of the mixtures are different. In the regime switching model, the log stock returns are modelled directly by a normal mixture conditioning on the underlying

market state variable. This results in a completely different density/distribution function than our lognormal mixture case as a linear mixture of exponentials differs from the exponential of a linear mixture. Moreover, the mixture weights in the regime switching model is subject to a Markov Chain process where a transition probability matrix P is involved and estimated. This is not the case in our MLN framework, where the mixing weights $\lambda_i, i \in \{1..N\}$ are treated as stable parameters implied by the market through the current derivative prices. To reflect any evolution of these parameters the whole model needs to be recalibrated by the technique suggested in Section 3.3.1. A detailed comparative study on the two models is not presented here

In conclusion, the approach we presented in the MLN model can be interpreted as consisting of multiple diffusions for the price process with different volatility parameters. Then we can choose among these diffusions with probability λ_i to capture the true market dynamic through the proposed calibration processes and consequently volatility changes randomly over time. Notice that this underlying procedure is exactly what a mixture distribution entails and we are taking full advantage of it. Since further knowledge about the corresponding price process is not necessary for the valuation of European options, this question is not addressed any further here.

Chapter 4

Pricing Exotic Options

The effectiveness of our MLN model for stable period index options is empirically discussed in the previous section. We now extend the framework to the pricing of exotic equity derivatives, which has been a popular subject of research in quantitative finance and actuarial risk management. Surprisingly, despite a large variation of mixture lognormal model specification, there is limited published literature on its application to exotic options. Admittedly, other complex models such as the simulated exponential Lévy's process[39] produce satisfactory results. However, most of them are numerically demanding. We now explore this topic under the MLN framework specified in Chapter 2. In particular, we derive closed-form pricing formulas for simple binary options and devise Black-Scholes style efficient simulation techniques for the pricing of path dependent options. These topics form a major portion of our contribution in this thesis.

4.1 Binary Options

A binary option is a European style option. It is also referred to as all or nothing option or, in the foreign exchange/interest rate market, a digital option. Depending on the payoff mechanics, there are two major categories of binary options:

1. Cash-or-nothing. For a call option, it pays the option holder a predefined amount Y if the underlying stock price exceeds the strike price K at option maturity and 0 otherwise. For a put option, the reverse is true.

2. Asset-or-nothing. For a call option, it pays the option holder the price of the underlying stock if it exceeds the strike price K at option maturity and 0 otherwise. For a put option, the reverse is true.

As before, we limit the scope of our discussion to call options only. In both categories, the call option holder receives nothing if the underlying stock price is below the strike price at maturity. Intuitively, the two types of binary options correspond to the two-components in the Black-Scholes option pricing formula (equation (2.12)), which will be shown below. The reason for this is that the strike price itself is not a deduction in the option payoff, which is solely based on the condition that the terminal underlying stock price exceeds the strike level. Under the MLN framework specified in Chapter 3, pricing formulas can be easily derived using partial expectations.

4.1.1 A Closed-form Pricing Formula under Mixture Lognormal Model

Similar to European options, closed-form pricing formulas are available for binary options and its derivation is quite straightforward. For cash-or-nothing call option, the terminal payoff is Y if $S(T) > K$ and 0 otherwise. Let BCC_{MLN} denote the price of this option under our MLN framework specified in Chapter 3 with risk neutral probability space (Ω, F, Q), components $(S_i, \lambda_i, \sigma_i)$, and current time $t = 0$. Assume a continuously compounded risk free rate of r and dividend rate of δ, we obtain the risk neutral price by taking the expected discounted payoff:

$$BCC_{MLN} = e^{-rT} E^Q[Y \mid S(T) > K] Q(S(T) > K)$$

As each component $S_i(t)$ follows the Black-Scholes framework, equations (2.8) and (2.9) apply. We also need to use an intermediary result in the alternative proof for Proposition 3.2.1 presented in Appendix B (equation (10)). This transforms the above equation to:

$$\begin{aligned} BCC_{MLN} &= e^{-rT} Y \sum_{i=1}^{N} Q(S_i(T) > K) \\ &= e^{-rT} Y \sum_{i=1}^{N} \lambda_i(d_2^i), \end{aligned} \tag{4.1}$$

where d_2^i denotes the d_2 quantity (defined by equation (2.11)) calculated using the parameters of the i^{th} component process, S_i.

Similarly, for asset-or-nothing call option, the terminal payoff is $S(T)$ if $S(T) > K$ and 0 otherwise. Let BAC_{MLN} denote the price of an asset-or-nothing call option under the MLN framework. In addition, based on Definition 2.1, Let $PE^+_{MLN,K}$ denote the partial expectation of S_T truncated from below at K under the MLN model and $PE^+_{i,K}$ denote the Black-Scholes partial expectation from the i^{th} component process. We apply the result in equation 9 of the alternative proof for Proposition 3.2.1 presented in Appendix B to obtain the arbitrage free price:

$$\begin{aligned} BAC_{MLN} &= e^{-rT} E^Q[S(T) \mid S(T) > K] Q(S(T) > K) \\ &= e^{-rT} PE^+_{MLN,K} \\ &= e^{-rT} \sum_{i=1}^{N} PE^+_{i,K}, \\ &= S_0 e^{-(r-\delta)T} \sum_{i=1}^{N} N(d_1^i) \end{aligned} \tag{4.2}$$

where the d_1^i denotes the d_1 quantity (defined by equation (2.10)) calculated using the parameters of the i^{th} component process, S_i. The last line above is the direct result of equation (2.8) as each component process is assumed to obey the Black-Scholes framework.

Now we have derived the binary option pricing formulas under our MLN model. By comparing them to the MLN pricing formula for call options in Proposition 3.2.1, it is quite apparent that each binary option is "half" of the regular call option depending on its type. The only deviation is that the payment amount Y may be (and usually is) different from the strike price K. Under the special case where there exists a pair of asset-or-nothing option and cash-or-nothing with cash payout $Y = K$ sharing the same maturity T and strike price K, a synthetic call option may be created by taking a long position in the former and a short position in the latter. This provides some insight in hedging strategies or portfolio constructions depending on the transaction costs associated with each type of option. Undoubtedly, it is desirable to choose the one with the least cost.

A second key observation is that the MLN binary option price of a binary option is simply a linear combination of Black-Scholes binary option prices from the components with corresponding weights. This result justifies the previous observation since the relationship between binary and call options (as we discussed) is well established under the

Black-Scholes model. We simply confirm that the same relationship holds under our MLN framework. This gives us the concluding proposition for this section of MLN binary option pricing formula.

Proposition 4.1.1: *Consider a binary option (call or put, cash-or-nothing or asset-or-nothing) under risk neutral pricing and the MLN model specified in Chapter 3. The stock price process $S(t)$ has mixing components $S_i(t)$ with corresponding weights λ_i and volatilities σ_i for $i \in \{1, 2, ...N\}$. The arbitrage free binary option price is equal to a linear combination of Black-Scholes binary option prices from the components weighed by the mixing weights.*

While the pricing formulas are given by equations (4.1) and (4.2), Proposition 4.1.1 clearly resonates with our previous results on European option pricing (Proposition 3.2.1) and Greek hedging (Proposition 3.2.2) under the our MLN framework. Again, numerical simplicity is a key advantage possessed by the MLN model compared to other complex approaches. Next, we propose an efficient calibration technique for the MLN binary option pricing model just established.

4.1.2 Calibration Technique and Empirical Example

The MLN binary option pricing model involves the same mixture parameters as the MLN model for European option pricing established previously. Therefore, the calibration procedure of minimizing the sum of square errors discussed in Section 3.3.1 is expected to be also a suitable approach for binary options. However, binary options are much less traded on the exchange, which implies that only limited market data is available for model calibration. Therefore, a better alternative approach is to estimate binary option parameters using the corresponding European option data. As the underlying stock paths remains the same, mixture parameters (e.g. mixing weights and component volatilities) do not vary among types of options. Therefore, this approach does not result in any methodological biases and can be further extended to price path dependent options as well.

As we have performed calibration of mixture parameters in Section 3.3.2 for the two-component MLN model, it suffices to demonstrate the concept using the same model and the same S&P500 index option data. We extract the calibrated parameters for the seven sample days and explore the pricing performances of the MLN model versus the traditional Black-Scholes model for binary cash-or-nothing call options. Notice that cash-or-nothing options are the only binary options for S&P500 traded on CBOE and all payment amounts

are equal to \$1 (e.g. $Y = 1$). The implied volatilities are not of a main concern to us in this extension of the MLN framework to exotic option pricing. Again, due to similarity of component volatility parameters given by stable period low volatility index levels, the pricing differences between our two-component MLN model and the Black-Scholes model is likely to be small. By the same procedure, we take the average of the bid-ask pair as the market option price and set $r = 2\%$. By applying the pricing formula in equation (4.1), we obtain the results as reported in Table 4.1 below. Recall that the Black-Sholes formula for a binary option is a simplified version of equation (4.1) obtained by setting $N = 1$, where, as before, N is the number of component processes in the MLN model.

		19-Jun	21-Jun	22-Jun	25-Jun	26-Jun	28-Jun	29-Jun
MLN Prices	$\mu(C)$	0.6043	0.5685	0.5733	0.5466	0.5581	0.5611	0.6050
	$\sigma(C)$	0.3924	0.4055	0.4081	0.4141	0.4133	0.4147	0.4132
	MSE	0.0018	0.0019	0.0015	0.0020	0.0021	0.0018	0.0015
	MAE	0.0376	0.0391	0.0399	0.0390	0.0388	0.0381	0.0338
	MPE	-2.06%	-8.42%	-9.68%	-14.47%	-13.94%	-13.76%	-10.17%
BS Prices	$\mu(C)$	0.6044	0.5685	0.5733	0.5466	0.5581	0.5612	0.6051
	$\sigma(C)$	0.3925	0.4056	0.4081	0.4141	0.4134	0.4146	0.4133
	MSE	0.0018	0.0019	0.0016	0.0020	0.0021	0.0019	0.0015
	MAE	0.0378	0.0392	0.0400	0.0391	0.0388	0.0382	0.0338
	MPE	-2.11%	-8.48%	-9.70%	-14.51%	-13.96%	-13.77%	-10.18%

Table 4.1: Performance of fitted MLN and Black-Scholes models for binary call

It is evident that qualitatively similar results are obtained as previously for European call options. No great improvement is observed from the MLN model over all seven sample days. A consistent conclusion is also implied by the aggregate data. The percentage pricing errors are plotted against spot-strike difference for both fitted models in Figure 4.1 below, which display extremely similar patterns as in the previous case for call options. Therefore, we conclude that the two-component MLN model does not yield much improvement over the standard Black-Scholes model in terms of pricing accuracy for S&P500 index binary options during stable market and low volatility periods.

4.2 Path Dependent Options: Asian Option

Asian options can be deemed as a fairly special case of path dependent options, where the option payoff directly depends on the average of the daily closing prices until option

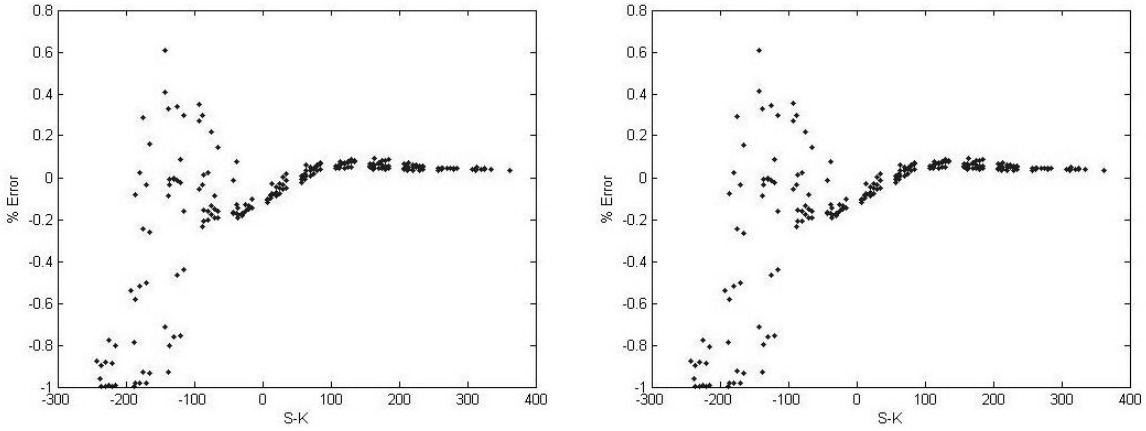

(a) Black-Scholes (b) MLN

Figure 4.1: Results for binary option pricing, percentage error vs. spot-strike difference

maturity. Unlike other path dependent options such as the barrier option, where variation in the underlying stock price of any particular day may render the option worthless, the averaging effect diminishes the impact of price changes over any single day. Consequently, price manipulative activities near option maturity has a less impact on Asian option prices. At the same time, just as most of the path dependent options, there is no closed-form pricing formula developed for Asian options. The difficulty lies in the fact that the average of lognormal random variables is not lognormally distributed[7], which is the key assumption for stock price under the Black-Scholes framework. The pricing is conducted through simulations, which we will present under our MLN model.

There are variations among Asian options. Most of them are European style without any possibility of early exercise but exceptions exist. For our purpose, only European style Asian options are considered. Let $\bar{S}(T)$ denote the average daily closing price until option maturity. An Asian option generally fall into one of the two categories below:

1. Average Strike Option: an average strike call option pays $(S(T) - \bar{S}(T), 0)^+$ and average strike put option pays $(\bar{S}(T) - S(T), 0)^+$ at option maturity.

2. Average Price Option: an average price call option pays $(\bar{S}(T) - K, 0)^+$ and average strike put option pays $(K - \bar{S}(T), 0)^+$ at option maturity, where K is the strike price

The term "average" may be refers to either an arithmetic mean or a geometric mean. This is specified for the Asian option contract. To avoid redundancy, we discuss the pricing for

the arithmetic average price call option only. Published literature on the pricing of Asian options is abundant. Chen and Lyuu (2007) derived a closed-form formula for the lower bound of arithmetic average Asian options (either average price or average strike) from the stochastic relationship between the time-t stock price and average stock price[7]. Other earlier literature focused on pricing the option directly, which includes the commonly used Monte Carlo simulation method in Boyle (1997)[3], Binomial Tree method in Hull and White (1993)[24], and approximation techniques using Taylor's expansion in Ju (2002)[26].

We present a Monte-Carlo simulation pricing technique under risk neutral pricing and the MLN model specified in Chapter 3, where the stock price conditionally follows a mixture lognormal distribution as defined in equations (3.13) and (3.14). This difference in distributional assumption is a fundamental difference between this approach and the Monte-Carlo method under the Black-Scholes framework. We will implement and compare the pricing results from the two-component mixture model in Section 3.2.3 and the one from the Black-Scholes framework. Accuracy will also be comparatively analyzed with the real market quote.

4.2.1 Pricing Technique with Simulation

Under the MLN framework specified in Chapter 3, we assume the stock price follows a continuous mixture diffusion path of N components. Therefore, the arbitrage-free price of an Asian average price call option under risk neutral measure (Ω, F, Q) is given by:

$$ACAP_{MLN} = e^{-rt} E^Q[(\frac{1}{T}\int_0^T S(t)dt - K)^+], \tag{4.3}$$

where $ACAP_{MLN}$ denotes the value of the option under the MLN framework and stands for "Asian call option, average price". By Definition 3.2.1, we decompose the integral expression into integral of components $S_i(t)$ to obtain:

$$ACAP_{MLN} = e^{-rt} \sum_{i=1}^{N} \lambda_i E^Q[(\frac{1}{T}\int_0^T S_i(t)dt - K)^+] \tag{4.4}$$

In reality, the average price is not calculated continuously. Rather, it is calculated in a discrete manner by taking the arithmetic average of the daily (or other periodically) closing

prices. This simplifies equation (4.3) and (4.4) above to:

$$ACAP_{MLN} = e^{-rt}E^{Q}[(\frac{1}{T}\sum_{j=1}^{T} S(j) - K)^{+}], \tag{4.5}$$

where we have discretized the stock price path so that $S(j)$ represents the closing price on day j. As mentioned previously, the distribution of the average term is difficult to derive under the Black-Scholes framework. It can be reasonably assumed that the same problem persists under our MLN model, which involves more complex mixture lognormal distributions. Therefore, we resort to Monte Carlo simulation in generating possible future stock price paths.

Under the Black-Scholes model, simulation is performed based on equation (2.3), where the Brownian motion takes randomly generated values from a standard normal distribution. By Definition 3.2.1 and equation (3.12) in our MLN model specifications, we obtain the equivalence of equation (2.3) under our MLN framework and risk neutral pricing with risk neutral probability space (Ω, F, P):

$$S(t) \mid (S_0, C = i) = S_0 e^{(r-\delta-\frac{1}{2}\sigma_i^2)(t)+\sigma_i\sqrt{t}Z(t)}, \tag{4.6}$$

where $Q(C = i) = \lambda_i$.

Based on this equation, we propose the following simulation based pricing procedure. To generate a single stock price path, we need to:

1. Fully calibrate the MLN parameters using the European Call option data for the same underlying stock. This is consistent with the approach for binary options and the calibration technique is discussed in Section 3.3.1.

2. For in-sample testing, the parameter time series may be used for sufficiently large time window. In practice, we need to simulate future price paths. Then we can either take the average over the time series for each parameter[1] or use the parameter estimates for the most recent day, whichever yields results that are more consistent with the economic/market trends. Notice that a subjective input is required here unless some external models are introduced.

[1]This includes the risk-free rate determined using the put-call parity condition as discussed in Section 3.3.1

3. To generate the next closing price from the current price, draw a value w_t from a standard normal distribution. This will be used as the shock $Z(t)$ value.

4. Determine which component process dominates. We do so by first partitioning the [0,1] interval to N subintervals whose lengths are proportional to the associated weight parameter λ_i. This creates a one-to-one matching between components and intervals. Randomly generate a number from a uniform [0,1] distribution. Choose the component whose interval this number falls into.

5. Suppose that component i dominates from step 4, compute the next closing price as:

$$S(t) = S_0 e^{(r-\delta-\frac{1}{2}\sigma_i^2)(t)+\sigma_i\sqrt{t}w_t}, \tag{4.7}$$

   where $t = \frac{1}{365}$ as we are averaging daily prices. Record this price and the corresponding date.

6. Shift the simulation window one day forward so that the price generated in step 4 enters the σ-algebra and is treated as the new S_0. Recursively perform steps 1-4 until we have reached and generated the maturity price.

For each price path, the option payoff is calculated as in equation (4.5). The fair price of the Asian average price call option is then the discounted mean of those payoff values. In our implementation, we shall produce 10000 price paths, which is sufficient for demonstration purpose. The option price is the discounted average of the payoffs produced under each simulated path.

There are several important elements that comprises the foundation of this simulation-based pricing method. First of all, it precisely implements the definitions and assumptions embedded in our MLN model, which is particularly pronounced in the modelling of mixture distribution by Definition 3.2.1. Secondly, it effectively applies the established Monte-Carlo simulation technique[3] for the Black-Scholes framework to each component, which, as discussed in Chapter 3, falls into the Black-Scholes case. Therefore, all rationales given by previous researchers on this topic serve well to justify our approach. Again, this is the main advantage of our MLN model over other complex exotic option models.

4.2.2 Pricing Example and Analysis

As Asian options are usually traded over-the-counter (OTC), there are no Asian option quotes available to us from the exchange data. Little information is given by other public

sources as well. Therefore, we do not have a data set of real market price as the benchmark for pricing precision analysis. In addition, we found in Section 3.3.2 that the S&P500 index option data sample does not yield component volatility parameters that are sufficiently different in magnitude to yield sharp demonstration. Therefore, we devise an example in a semi-hypothetical setting, where the calibrated parameters are preset. We will only focus on the pricing differences (if any) between the MLN model and Black-Scholes model to examine any possible improvements of our MLN model.

Example 4.2.2: pricing average price Asian call options

The SP500 index reaches \$1357.98 at the end of June 19, 2012. Assume that the following average price Asian call options are traded:

1. *APAC with K=1520 maturing in 60 days,*
2. *APAC with K=1350 maturing in 60 days,*
3. *APAC with K=1210 maturing in 60 days,*
4. *APAC with K=1410 maturing in 120 days,*
5. *APAC with K=1410 maturing in 365 days,*
6. *APAC with K=1410 maturing in 547 days,*

where the price average is calculated from daily closing prices. The risk free interest rate is $r = 0.02$ *and the stock pays no dividend. Suppose that, through the calibration process in Section 3.3.2 using European option quotes on the index, we obtain the following parameter estimates:*

1. *under the Black-Scholes model:* σ*=0.27,*
2. *under the two-component MLN model:* σ_1*=0.15,* σ_2*=0.45, and* λ*=0.65*

We would like to price the above 6 options using both the MLN and the Black-Scholes models.

Notice that in this semi-hypothetical setting, we deliberately choose volatility values so that the weighted average of the component volatilities under the two-component MLN

model stays close to the single volatility in the Black-Scholes model[2]. This forms a relatively fair basis for model comparison. We would like to see if the independent existence of the downside and upside component introduces significant effect in the produced Asian call option prices. Using the simulation based methodology discussed previously in Section 4.2.2. we generate 100 prices per option. The result is summarized in Table 4.2 below, where the statistics is organized by strike-maturity combinations and the last row contains the percentage differences between the mean option prices given by the two models.

$K-T$	Comb.	1520-60	1350-60	1210-60	1410-120	1410-365	1410-547
	Mean	3.1411	48.3368	160.5432	37.2577	79.4346	102.4843
MLN	Std.	0.1786	0.6909	0.9382	0.6112	1.4617	1.6330
Prices	Max	3.6512	50.5248	163.1176	38.5183	82.9906	106.6586
	Min	2.7183	46.4855	158.9941	36.0075	75.2663	99.0957
	Mean	2.1332	45.5134	160.4397	33.2391	72.4691	95.6772
BS	Std.	0.1341	0.5945	0.8972	0.6049	1.2386	1.5424
Prices	Max	2.5129	47.5565	163.1366	34.6224	76.2676	98.3991
	Min	1.8119	44.1810	157.8285	31.8432	69.3904	90.7806
% Mean	Dif.	47.24%	6.20%	0.31 %	12.09 %	9.61%	7.11 %

Table 4.2: Performance of MLN and Black-Scholes models for Asian call

Several key conclusions can be drawn from the results. Firstly, the variances in prices given by the MLN model exceed the ones produced by the Black-Scholes model for all 6 options. This is consistent with our expectation as the mixture distribution contains more uncertainly than the single lognormal distribution. Secondly, the Black-Scholes prices for all options fall below their counterparts from the MLN model. Though it may be biased from the relationship we imposed on the volatility parameters, some general trends do emerge: For the same time to maturity, difference in the mean option prices decrease as option becomes in-the-money[3] (see results for the first 3 options). For the same strike price, such difference slightly decreases as time to maturity increases (results for the last 3 options).

While both phenomenon can be well explained, we start from the first option, where

[2]We do so to construct a fair model comparison basis, which is ideally done through calibration. The implication for using the weighted average volatility as an approximation is given by the previous result in Table 3.4. Working with equation (3.29) is not an alternative as it yields approximated implied volatilities.

[3]We use "in-the-money" or "out-of-the-money" to refer to the relationship of the spot underlying stock price and the strike price only. Their precise definitions for Asian options include the average stock price and is not what we mean here.

the difference is most pronounced. We have strike price $K = 1520$ and time to maturity $T = 60$ days. Taking into account the low interest rate and thus small risk-neutral drift term, this option is significantly out-of-the-money and close to maturity. In order for the option to generate a non-zero maturity payoff, it needs to go through a series of significant upward jumps before expiration, which is easier to achieve under the MLN case due to the existence of the upside component $S_2(t)$. When this happens, the two-component mixture mimics Merton's Jump Diffusion process(See Leisen (2004)[29]). The sensitivity to the downside component $S_1(t)$ is small as the option is deeply out-of-the money and the magnitude of maturity moneyness is irrelevant if the option expires with no payoff. However, the downside component becomes more effective in offsetting the high volatility momentum as the option becomes more deeply in-the-money ($K = 1210$), where each movement, whether up or down, is equally significant in affecting the maturity payoff. This explains the first trend, which is also illustrated by Figure 4.2 below. The vertical axis represents the percentage price difference calculated as

$$\frac{APAC_{MLN} - APAC_{BS}}{APAC_{MLN}},$$

and the horizontal axis is the option number. While $T = 60$ days for all plotted options, options 1 to 100 have $K = 1520$, options 101-200 have $K = 1350$, and options 200 to 300 share $K = 1210$. The three distinct regions clearly display a stepwise decreasing pattern as we expect.

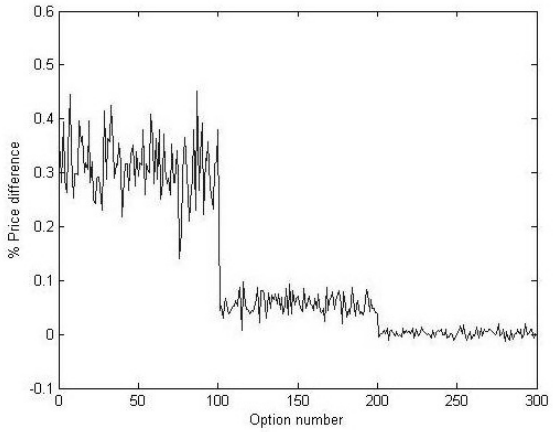

Figure 4.2: APAC price differences under MLN and BS models, fixed maturity

The second trend is also intuitive. The effects of both components diminish systematically when the average price is taken on a larger pool of daily closing prices brought by a longer time to maturity. Notice that the first trend is also visible in the last three options. As they are all out-of-the money, the one with the least maturity has the largest mean price difference to its Black-Scholes counterpart.

Therefore, we see that under the two component MLN model, the downside component does not exert significant momentum of crash-o-phobia effect to Asian options. Even when its existence is significant ($\lambda > 0.5$ and thus the expectations $S_t^1 < S_t < S_t^2$), the effect is offset by the price averaging nature of Asian options as well as the effect of the upside component. The jump-diffusion nature of the MLN model makes near-maturity out-of-the money call options more expensive than their corresponding Black-Scholes prices. In spite that no real market quotes is available for accuracy comparison, the observations can be utilized for hedging purposes. For instance, a short position in a near maturity out-of-the-money Asian call should be conservatively hedged using the MLN model to prevent unexpected losses.

4.3 Path Dependent Options: Barrier Option

In contrast to Asian options, Barrier options are regular Call or Put options with an underlying stock price barrier or trigger level that either must be met or must be avoided for the option to be active at maturity. Almost all barrier options are European style. As a result, the price of a barrier option must be less than that of its European counterpart. Under the broad category of Call or Put options, there are four types of barrier options:

1. up-and-out options: the option becomes worthless if the underlying stock attains a price above the barrier some time before maturity. Otherwise it functions as a European option.

2. down-and-out options: the option becomes worthless if the underlying stock attains a price below the barrier some time before maturity. Otherwise it functions as a European option.

3. up-and-in options: the option becomes active as an European option if and only if the underlying stock attains a price above the barrier some time before maturity. Otherwise it pays nothing at maturity.

4. up-and-in options: the option becomes active as an European option if and only if the underlying stock attains a price below the barrier some time before maturity. Otherwise it pays nothing at maturity.

The former two types of barrier options are commonly referred to as "knock-out options" while the latter two are "knock-in options". Once the option is knocked-out, it immediately becomes worthless and there is no means of reversal. On the other hand, once the option is knocked-in, it remains effective regardless of future price movement. Therefore, any jump in price may incur a huge impact on the option value. Though stock prices are modelled by continuous stochastic paths under the Black-Scholes framework as well as in our MLN model, in practice, the price is usually discretely measured at fixed time steps. Discrete price monitoring brings difficulty to barrier option pricing. In particular, it does not allow the development of a closed-form formula as in the case of continuous price unless m-dimensional Brownian motions are used, where m is the number of monitoring points(See Kou (2003)[27]). The complexity of such a model can be reasonably envisioned. On the other hand, barrier options with continuously monitored underlying stock price is a classic topic fist studied by Merton(1973)[33], who derived the analytical pricing formula for a down-and-out put option. Subsequent research by Reiner and Rubinstein (1991)[36] refined Merton's work and further proposed closed-form formulas for all 8 possible types of Barrier options by solving Black-Scholes PDEs with additional barrier conditions. These formulas are shown in Appendix E. We do not review the detailed derivation as it is far more complex than that of the Black-Scholes model reviewed in Chapter 1. For barrier options with discrete price measurements, pricing is commonly performed through Monte Carlo simulation as we introduced for Asian options.

Nevertheless, all those pricing formulas and techniques are base on the Black-Scholes framework, where the stock price follows a single diffusion process described by equation (2.1). We now devise a pricing formulas and methodologies under our MLN model introduced in Chapter 3, where the price dynamic is described by a mixture diffusion process (equation (3.3) to (3.7)). We then implement the techniques using the same S&P500 data and the two-component mixture model as before and compare the pricing results to those produced under the Black-Scholes framework.

4.3.1 Pricing Formulas and Simulation-based Pricing Methodology

The pricing of Barrier options, whether continuously or discretely monitored, can be substantially simplified by identifying the properties and parity conditions embedded in the option payoff. Those properties are commonly used under the Black-Scholes framework. However, as the derivation is based on the option payoff at maturity, they also hold true under our MLN model.

Let H denote the barrier of the option and K the strike price as usual. An up-and-out call option with $H \leq K$, which has no value as the option is knocked out before it ever becomes in the money. As a result, it has a price of 0. Similar argument applies to a down-and-out put option with $H > K$. Notice that if we categorize all possible options by the relationship between H and K combined with call/put type, we will have a total of 16 cases. The simple result under these two special cases saves a lot of derivation efforts.

In addition to the two special cases above, consider an up-and-in call option with $H \leq K$. The barrier is satisfied automatically if the call option ever becomes in-the-money. If not, the option has no payoff and barrier is thus of no concern. Therefore, the barrier in this case is ineffective and the option functions exactly the same way as a regular European call option, meaning its no-arbitrage price is equal to that of its European option counterpart. Similar argument applies to a down-and-in put option with $H > K$. These two cases further simplifies the derivation of formula.

Lastly, consider taking long positions in a pair of down-and-in call and down-and-out call options with the same barrier, strike price, and maturity. Clearly, exactly one of these two options will stay effective at maturity and the payoff is identical to that of an equivalent European call option. To guarantee no arbitrage, we have the following relationship:

$$C_{DI} + C_{DO} = C_{BS}, \tag{4.8}$$

where the subscript DI and DO represent the barrier type (e.g. "down-and-in" and "down-and-out" respectively).

Such a relationship is known as barrier option in-out parity. By the same argument,

the other three parities can be easily obtained:

$$C_{UI} + C_{UO} = C_{BS}, \tag{4.9}$$
$$P_{DI} + P_{DO} = P_{BS}, \tag{4.10}$$
$$P_{UI} + P_{UO} = C_{BS}, \tag{4.11}$$

where the subscript UI and UO also represent the barrier type (e.g."up-and-in" and "up-and-out" respectively).

All of these three major properties are used in Reiner and Rubinstein (1991)[36], where the closed-form formulas for continuously monitored barrier option prices are derived. We summarized these key results and presented them in Appendix E. As those formulas are built under the Black-Scholes framework, the following proposition extends its application to continuously monitored barrier options under our MLN framework.

Proposition 4.3.1: *Consider a continuously monitored barrier option (either call or put, knock-in or knock-out) under risk neutral pricing and the MLN model specified in Chapter 3. The stock price process $S(t)$ has mixing components $S_i(t)$ with corresponding weights λ_i and volatilities σ_i for $i \in \{1, 2, ...N\}$. The arbitrage free barrier option price is equal to a linear combination of Black-Scholes barrier option prices from the components weighed by the mixing weights.*

Similar to previous propositions, we prove the result by conditioning on the underlying mixture state variable C. Without loss of generality, it suffices to present the proof for an down-and-in call option only. Define binary indicator variable 1_A, which takes value of 1 if event A is holds and 0 otherwise. Also define the following quantity:

$$\xi(S, H) = \inf\{t | t \geq 0, S(t) < H\}.$$

Under risk-neutral pricing with probability space (Ω, F, Q), the price of this down-and-in call option is equal to the expected discounted value of its payoff. We add the superscript

to indicate which framework the pricing is based on. This gives us:

$$\begin{aligned} C_{DI}^{MLN} &= E^Q[e^{-rT}(S(T)-K)^+ 1_{\xi(S,H)<T}] \\ &= E^Q[e^{-rT}E[(S(T)-K)^+ 1_{\xi(S,H)<T} \mid C]] \\ &= e^{-rT}\sum_{i=1}^{N} E^Q[(S_i(T)-K)^+ 1_{\xi(S_i,H)<T} \mid C=1]Q(C=i) \\ &= \sum_{i=1}^{N} \lambda_i E^Q[e^{-rT}(S_i(T)-K)^+ 1_{\xi(S_i,H)<T}] \\ &= \sum_{i=1}^{N} \lambda_i C_{DI}^{BS,i}, \end{aligned} \tag{4.12}$$

where $C_{DI}^{BS,i}$ denotes the continuously monitored down-and-in option price under the Black-Scholes model using parameters from component process $S_i(t)$. This proves Proposition 4.3.1 above. Therefore, we have obtained closed-form pricing formulas for all continuously monitored barrier options under our MLN framework. The fully extended forms of these formulas are obtained by substitutions of the relevant Black-Scholes barrier option formulas in Appendix E. We do not demonstrate this trivial step here.

For discretely measured barrier options, we propose a simulation based pricing technique. The simulation procedure is the same as the one proposed in Section 4.2.1 for Asian options except for the calculation of payoff. The modification is added after step 6 of the simulation process, where, for each simulated stock path, we determine if the barrier option of interest is knocked-in or knocked-out at monitoring points and calculate the maturity payoff accordingly. The price of the option is the discounted average of the maturity payoffs produced by each simulated price path. Again, for demonstrative purpose, we generate 10000 stock price path when pricing each option. Also, we assume the underlying stock price is monitored at the end of every 3 days.

4.3.2 Pricing Example and Analysis

In this section, we show the application of the pricing formulas and techniques for barrier options proposed in the previous section. We provide the example for pricing down-and-in call options. As discussed in the previous section, closed-form formulas are available for

continuously monitored options only and simulation-based technique is used when pricing discretely monitored barrier options. We illustrate the result under each of the two scenarios. Similar to Asian options, real market quotes for barrier options are not available to us, indicating the absence of a comparative basis for pricing accuracy. To emphasize the difference (if any) in pricing results by the two models, we use the same assumed parameters as in our demonstration for Asian options

Example 4.3.2: pricing down-and-in barrier call options

The SP500 index reaches \$1357.98 at the end of June 19, 2012. Assume that the following down-and-in barrier call options are traded:

1. C_{DI} *with K=1520 maturing in 60 days,*
2. C_{DI} *with K=1350 maturing in 60 days,*
3. C_{DI} *with K=1210 maturing in 60 days,*
4. C_{DI} *with K=1410 maturing in 120 days,*
5. C_{DI} *with K=1410 maturing in 365 days,*
6. C_{DI} *with K=1410 maturing in 547 days,*

The barrier is $H = 1300$ *for all 6 options. The risk free interest rate is* $r = 0.02$ *and the stock pays no dividend. Suppose that, through the calibration process in Section 3.3.2 using European option quotes on the index, we obtain the following parameter estimates:*

1. *under the Black-Scholes model:* σ*=0.27,*
2. *under the two-component MLN model:* σ_1*=0.15,* σ_2*=0.45, and* λ*=0.65*

We would like to price the above 6 options using both the MLN and Black-Scholes models under two different scenarios:

1. *the barrier options are monitored continuously,*
2. *the barrier options are monitored at the end of every 3 trading days,*

and compare the results obtained.

The first scenario allows us to apply closed-form formulas directly. We implement the extended formulas obtained by applying Proposition 4.3.1 and the Black-Scholes barrier option pricing formulas in Appendix E. The result is summarized in Table 4.3 below.

$K-T$ Comb.	1520-60	1350-60	1210-60	1410-120	1410-365	1410-547
C_{DI}^{MLN}	6.4971	21.1975	67.9332	28.6990	79.7177	110.7492
C_{DI}^{BS}	2.2038	20.1638	74.6123	26.6403	84.3119	118.8180
% Dif.	66.08%	4.88%	-9.83 %	7.17 %	-5.76%	-7.29 %

Table 4.3: Performance of MLN and Black-Scholes models for continuous barrier call

While a fairly small price sample is produced by the two models for comparison, some key observations can be made readily.

First of all, the near maturity deeply out-of-the-money[4] option is priced substantially higher by the MLN model as exemplified by the first option with $K = 1520$ and $T = 60$ days, which is similar to what we observed for Asian average price call options priced by our proposed simulation method. This effect is magnified by the knock-in barrier of $H = 1300$, which is much smaller than the strike price. To produce a positive payoff, the stock price must dive below the barrier and rise above the strike price at maturity. Such paths are more likely under the MLN model, which, as discussed previously, is capable of producing the jump-diffusion pattern due to the existence of the volatile upside component $S_2(t)$. The downside component is least effective here. However, as the option becomes in the money, the barrier becomes the only concern and the jump-diffusion is less valued. As a result, the downside component exerts more momentum due to its heavier weights. This decreases the MLN prices to levels below their Black-Scholes counterparts as shown by the table. Unlike Asian options, where averaging effects takes part in offsetting the contradicting forces from the two MLN components, any price difference is pronounced in this case, as demonstrated by the first three options in the table.

Secondly, the same pattern propagates as time to maturity increases, which is shown by the last three options sharing the same strike price and barrier. The main reason is that the requirement for jump-diffusion is less when a longer time to maturity remains, putting the more heavily weighted downside component into a dominant position. A significant

[4]Similar to the Asian option case, we use moneyness in describing the spot-strike relationship only.

positive price difference exist for the fourth option with $K = 1410$ and $T = 60$ days. The argument is exactly the same as the one for the first option. However, as moneyness is less nagative and distance to barrier is smaller in this case, the MLN price exceeds the Black-Scholes price by a smaller amount.

Notice that the rationales here for the observed patterns are more systematic and firmly established compare to the ones drawn for Asian options. Moreover, recall that for Asian options, though the MLN prices decrease and move toward their Black-Scholes counterparts in the same $K - T$ patterns observed here for binary options, the MLN prices never fall below the corresponding Black-Scholes prices. This is not true in our barrier option case, where the MLN prices can decrease in the identified pattern and eventually fall below their Black-Scholes counterparts. This is most likely caused by the fundamental difference in option mechanics.

Our results above show that continuously monitored down-and-in call options are sensitive to crash-o-phobia effects. We now examine if the same argument hold for discretely monitored barrier options. To price theses options, we implement the same simulation based technique as for Asian options introduced in Section 4.2.1. Similar to our analysis for Asian options, we price each of the six barrier options 100 times to using each model to obtain a summary statistics for the produced prices. The results are presented in Table 4.4 below.

$K - T$	Comb.	1520-60	1350-60	1210-60	1410-120	1410-365	1410-547
	Mean	1.6578	14.3183	54.9675	22.2282	79.7520	110.1820
MLN	Std.	0.1448	0.4388	0.8090	0.6971	1.7417	2.6866
Prices	Max	1.9863	15.2823	57.2432	23.6008	83.7797	121.1133
	Min	1.3824	13.3226	52.3798	20.5401	75.7857	107.8225
	Mean	1.0847	12.6478	55.9777	18.9996	70.9619	104.3091
BS	Std.	0.1091	0.4289	0.7749	0.6118	1.7033	2.2628
Prices	Max	1.3399	13.7219	56.8648	20.6072	74.5928	109.8326
	Min	0.8430	11.7010	52.8357	17.5872	66.5029	99.9039
% Mean	Dif.	34.57%	11.67%	-1.84 %	14.52 %	11.02%	9.44 %

Table 4.4: Performance of MLN and Black-Scholes models for discrete barrier call

Observe that the mean option prices are generally lower than prices of the continuously monitored down-and-in call options in Table 4.3. This is expected as less frequent mon-

itoring decreases the chance that the option gets knocked in. Exceptions are option 5 and 6 from the MLN model, where the prices are similar to those from the continuous cases. This can be partially explained by the long maturities these two options possess, which means that there is a small chance that they stay above the barrier. Also notice that under this discrete case, the relationship between price levels, strike price, and maturities resemble what we observed previously for Asian options in Section 4.2.2. The differences between each pair of MLN and Black-Scholes prices decrease as option become in-the-money and as time to maturity increases. However, rarely do the MLN price fall below their Black-Scholes counterparts. This implies that for discretely monitored barrier options, the crash-o-phobia effect implied by the downside component is overcome by the combined effect of jump-diffusion and high mixture volatility brought by the upside component, especially for long maturities. This is a departure from the patterns observed for continuously monitored barrier options. On the other hand, such a departure does not give rise to a contradiction. Figure 4.3 below shows the percentage differences between all MLN and Black-Scholes prices for the first three options, where maturity is fixed at $T = 60$ days. The options are numbered so that prices 1 to 100 correspond to option 1 with $K = 1520$, prices 101 to 200 correspond to option 2 with $K = 1350$, etc.

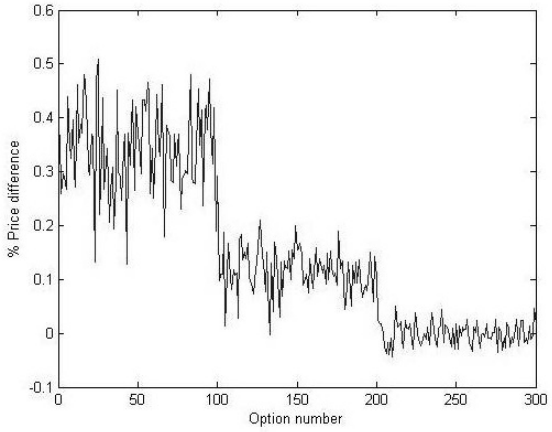

Figure 4.3: C_{DI} price differences under MLN and BS models, fixed maturity

Notice that similar to Figure 4.2 for Asian call options, 3 decreasing regimes are easily identified. This suggests similar implications for hedging barrier options, where short positions in near maturity out-of-the-money calls are conservatively hedged using the MLN model. Again, pricing accuracy is beyond our study in this case.

Chapter 5

Conclusion

In conclusion, we have examined the main properties of the mixture lognormal option pricing model. We started the analysis by specifying the mixture diffusion process followed by the stock price path and extend the result to define and form a general MLN model for stock price with time-invariant component volatilities. Closed-form formulas are derived for European style options under our MLN framwork based on the proved propositions that option prices under the mixture model are linear combinations of the corresponding Black-Scholes prices.

The two-component mixture, as the simplest MLN model, is closely studied and empirically demonstrated through an application to S&P500 index options under a relatively tranquil and stable volatility period. It appears that though significant existence of crash-o-phobia parameters is evident, the individual component volatilities do not differ much from each other, delivering only minimal improvements in pricing accuracy from our MLN model over the Black-Scholes model. This departs from the results in previous researches applying the mixture model to turbulent period stock options. Nevertheless, we found that the capability of producing the desired volatility smiles is preserved as the difference between component volatilities widens in magnitude, meaning the downside component $S_1(t)$ plays a critical role in generating the volatility skews from market information, and the two-component model is sufficient for capturing this feature.

As a major contribution of this thesis, we extended our MLN model to price exotic options. We found that binary options for tranquil period stock index are not priced at a significant better accuracy under the MLN model for the same reason of similarity in component volatilities. This is expected to be improved for volatile period markets or

individual stocks. We proposed simulation-based pricing methodology for Asian options and discretely monitored barrier options. It is found that call options are priced higher by our MLN model compared to the Black-Scholes prices due to the jump-diffusion nature of our mixture model brought by the high-volatility upside component $S_2(t)$. The magnitude of this difference decreases as time to maturity or moneyness increases. This same trend also prevails for continuously monitored barrier call options, where closed-form formulas are available. Nevertheless, crash-o-phobia and effect of the downside component are more pronounced so the MLN prices fall below the Black-Schole prices for options with long maturities. These unique features provides insights in the formulation of risk management portfolios, where the MLN model should be used to create conservative hedging strategies for short positions in these exotic options.

Overall, our MLN model is an effective option pricing tool for assets during high volatility period, especially when stylized return patterns are evident. The volatility smile problem is well resolved by this framework. For future work, extensions and more empirical study of the model on various financial derivatives traditionally priced under the Black-Sholes model is desired.

APPENDICES

This section contains proofs, formulas, and other supplemental material that facilitates the comprehension of key concepts presented in the thesis.

Appendix A

Proof of Proposition 3.1

The Fokker Plank equation applies to diffusion processes in the following form:

$$dX_t = D_1(X_t, t)dt + \sqrt{2D_2(x_t, t)}dZ(t), \tag{A.1}$$

Let $f(x,t)$ denote the density function of X_t. The Fokker-Plank equation states that the following holds true for all defined $t \in R^+$:

$$\frac{\partial}{\partial t}f(x,t) = -\frac{\partial}{\partial x}\left[D_1(x,t)f(x,t)\right] + \frac{\partial}{\partial x}\left[D_2(x,t)\frac{\partial}{\partial x}f(x,t)\right]. \tag{A.2}$$

Apply equation (A.2) to equation (3.1) and (3.2), we get:

$$\frac{\partial}{\partial t}f(S,t) = -\mu S\frac{\partial}{\partial s}f(S,t) + \frac{1}{2}\sigma^2(S,t)S^2\frac{\partial^2}{\partial S^2}f(S,t) \tag{A.3}$$

$$\frac{\partial}{\partial t}f_i(S,t) = -\mu_i S\frac{\partial}{\partial S}f_i(S,t) + \frac{1}{2}\sigma_i^2 S^2\frac{\partial^2}{\partial S^2}f_i(S,t),\ i \in 1,2..N. \tag{A.4}$$

Now, multiply both sides of equation (A.4) by the mixture weight λ_i and take summation for $i \in 1,2,..N$, we obtain equation (A.5) below by the linearity of partial differentiations:

$$\frac{\partial}{\partial t}\sum_{i=1}^{N}\lambda_i f_i(S,t) = -S\frac{\partial}{\partial S}\sum_{i=1}^{N}\lambda_i\mu_i f_i(S,t) + \frac{1}{2}S^2\frac{\partial^2}{\partial S^2}\sum_{i=1}^{N}\lambda_i\sigma_i^2 f_i(S,t),\ i \in 1,2..N. \tag{A.5}$$

If all drifts terms are set to be equal, that is to say, $\mu = \mu_i,\ \forall i \in 1, 2..N$, equation (A.5) is simplified by factoring out the drift term from the summation:

$$\frac{\partial}{\partial t}\sum_{i=1}^{N}\lambda_i f_i(S,t) = -\mu S\frac{\partial}{\partial S}\sum_{i=1}^{N}\lambda_i f(S,t) + \frac{1}{2}S^2\frac{\partial^2}{\partial S^2}\sum_{i=1}^{N}\lambda_i\sigma_i^2 f_i(S,t),\ i \in 1, 2..N. \quad \text{(A.6)}$$

By the definition of the mixture diffusion process in equation (3.4), we know that

$$f(S,t) = \sum_{i=1}^{N}\lambda_i f(S,t),$$

and therefore equation (A.6) is further simplified to:

$$\frac{\partial}{\partial t}f(S,t) = -\mu S\frac{\partial}{\partial S}f(S,t) + \frac{1}{2}S^2\frac{\partial^2}{\partial S^2}\sum_{i=1}^{N}\lambda_i\sigma_i^2 f_i(S,t), \quad \text{(A.7)}$$

Matching equation (A.7) with equation (A.3), it is apparent that:

$$\frac{1}{2}S^2\sigma^2(S,t)\frac{\partial^2}{\partial S^2}f(S,t) = \frac{1}{2}S^2\frac{\partial^2}{\partial S^2}\sum_{i=1}^{N}\lambda_i\sigma_i^2 f_i(S,t), \quad \text{(A.8)}$$

Integrate twice both sides of the equation with respect to t and solve for $\sigma^2(s,t)$ to get

$$\sigma(S(t),t) = \sqrt{\frac{\sum_{i=1}^{N}\lambda_i\sigma_i^2 f_i(S(t),t)}{\sum_{i=1}^{N}\lambda_i S(t)^2 f_i(S(t),t)}}, \quad \text{(A.9)}$$

which is exactly as we stated in equation (3.6).

Appendix B

Proof for Proposition 3.2.1 Using Partial Expectations

Similar to equation (2.7) in the review of the Black-Scholes Framework, using risk neutral pricing:

$$\begin{aligned} C_{MLN} &= E^Q[(e^{-rT}(S(T)-K)^+] \\ &= e^{-rT}E^Q[(S(T)-K)^+] \\ &= e^{-rT}E^Q[S(T)-K \mid S(T)>K]Q(S(T)>K) \\ &= e^{-rT}[PE_K^+(S(T)) - KPr(S(T)>K)]. \end{aligned} \tag{B.1}$$

The MLN framework is as defined in Section 3.1 and Section 3.2.1. To simplify the notation, we ignore $S(T)$ in the notation by treating it as the default variable of interest unless otherwise specified. Based on definition 2.1, Let $PE^+_{MLN,K}$ denote the partial expectation of S_T truncated from below at K under the MLN model and $PE^+_{i,K}$ denote the Black-Scholes partial expectation from the i^{th} component process. Also, let $f(s)$ denote the density function for $S(T)$ and $f_i(s)$ the density function for mixing component $S_i(T)$, with $F(s)$ and $F_i(s)$ being the corresponding distribution function. Then, by equation (3.11),

we have

$$\begin{aligned} PE^{+}_{MLN,K} &= \int_K^\infty sf(s)ds = \int_K^\infty s\sum_{i=1}^N \lambda_i f_i(s)ds \\ &= \sum_{i=1}^N \lambda_i \int_K^\infty sf_i(s)ds \\ &= \sum_{i=1}^N \lambda_i PE^{+}_{i,K}. \end{aligned} \tag{B.2}$$

Similarly, by equation (3.10), we have:

$$\begin{aligned} Q(S(T) > K) &= 1 - F(K) = 1 - \sum_{i=1}^N \lambda_i F_i(K) \\ &= 1 - \sum_{i=1}^N \lambda_i (1 - Q(S_i(T) > K)) \\ &= 1 - 1 + \sum_{i=1}^N \lambda_i Q(S_i(T) > K) \\ &= \sum_{i=1}^N \lambda_i Q(S_i(T) > K). \end{aligned} \tag{B.3}$$

Equations (B.1) to (B.3) give:

$$\begin{aligned} C_{MLN} &= E^Q[(e^{-rT}(S(T) - K)^+] \\ &= e^{-rT}[PE^{+}_{MLN,K} - KQ(S(T) > K)] \\ &= e^{-rT}[\sum_{i=1}^N \lambda_i PE^{+}_{i,K} - K\sum_{i=1}^N \lambda_i Q(S_i(T) > K)] \\ &= \sum_{i=1}^N \lambda_i e^{-rT}(PE^{+}_{i,K} - KQ(S_i(T) > K)) \\ &= \sum_{i=1}^N \lambda_i C^i_{BS}, \end{aligned} \tag{B.4}$$

which is what we expect from Proposition 3.2.1. The proof for put option requires only a trivial modification on the payoff functions and the type of partial expectation involved.

Appendix C

Formula for European Option Greeks under Black-Scholes Framework

For an European stock option with time to maturity T and strike price K, let S denote the initial/current stock price, r the continuously compounded risk free rate, and δ the continuously compounded dividend rate. The option Greeks can be calculated via the following formulas [21]:

Greek	Call option	Put option
Δ	$e^{-\delta T}N(d_1)$	$-e^{-\delta T}N(-d_1)$
γ	$e^{-\delta T}\frac{N^{'}(d_1)}{S\sigma\sqrt{T}}$	$e^{-\delta T}\frac{N^{'}(d_1)}{S\sigma\sqrt{T}}$
θ	$\frac{-e^{-\delta T}SN^{'}(d_1)\sigma}{2\sqrt{T}} - rKe^{-rT}N(d_2) + \delta Se^{-\delta T}N(d_1)$	$\frac{-e^{-\delta T}SN^{'}(d_1)\sigma}{2\sqrt{T}} + rKe^{-rT}N(-d_2) - \delta Se^{-\delta T}N(-d_1)$
ρ	$KTe^{-rT}N(d_2)$	$-KTe^{-rT}N(-d_2)$
ψ	$-STe^{-\delta T}N(d_1)$	$-STe^{-\delta T}N(-d_1)$
ν	$Se^{-\delta T}N^{'}(d_1)\sqrt{T}$	$Se^{-\delta T}N^{'}(d_1)\sqrt{T}$

Table C.1: Black-Scholes formulas for option Greeks

where d_1 and d_2 are specified in equations (2.10) and (2.11) and we repeat here for conve-

nience:

$$d_1 = \frac{\ln(\frac{S}{K}) + (r - \delta + \frac{1}{2}\sigma^2)T}{\sigma\sqrt{T}},$$
$$d_2 = \frac{\ln(\frac{S}{K}) + (r - \delta - \frac{1}{2}\sigma^2)T}{\sigma\sqrt{T}} = d_1 - \sigma\sqrt{T},$$

and

$$N^{'}(d_1) = \phi(d_1) = \frac{e^{\frac{-d_1^2}{2}}}{\sqrt{2\pi}}.$$

Appendix D

Proof for Proposition 3.2.3

We prove this proposition by conditioning on the state variable C underlying the mixture process.

$$\begin{aligned}
Var_t(S(T)) =& E_t[Var_t(S(T) \mid C)] + Var_t(E_t[S(T) \mid C]) \\
=& (Var(S_1(T))\lambda + Var(S_2(T))(1-\lambda)) \\
&+ (E[S_1(T)]^2\lambda + E[S_2(T)]^2(1-\lambda)) \\
&- (E[S_1(T)]\lambda + E[S_2(T)](1-\lambda))^2 \\
=& \lambda Var(S_1(T)) + (1-\lambda)Var(S_2(T)) + \lambda E[S_1(T)]^2 \\
&+ (1-\lambda)E[S_2(T)]^2 - \lambda^2 E[S_1(T)]^2 - (1-\lambda)^2 E[S_2(T)]^2 \\
&- 2\lambda(1-\lambda)(E[S_1(T)]E[S_2(T)]) \\
=& \lambda Var(S_1(T)) + (1-\lambda)Var(S_2(T)) + \lambda(1-\lambda)E[S_1(T)]^2 \\
&- \lambda(1-\lambda)E[S_2(T)]^2 - 2\lambda(1-\lambda)(E[S_1(T)]E[S_2(T)]) \\
=& \lambda Var(S_1(T)) + (1-\lambda)Var(S_2(T)) + \lambda(1-\lambda)(E[S_1(T)] - E[S_2(T)])^2,
\end{aligned}$$

which is exactly what we proposed.

Appendix E

Formula for Continuously Monitored Barrier Option Prices under Black-Scholes Framework

The following pricing formulas for continuously monitored barrier options are summarized and adapted from Reiner and Rubinstein (1991)[36]. Let H denote the barrier level, we define the following quantities:

$$
\begin{aligned}
m &= \frac{r - \delta + 0.5\sigma^2}{\sigma^2}, \\
y &= \frac{\ln(\frac{H^2}{S_0 K})}{\sigma\sqrt{T}} + m\sigma\sqrt{T}, \\
z &= \frac{\ln(\frac{H}{S_0})}{\sigma\sqrt{T}} + m\sigma\sqrt{T}, \\
x &= \frac{\ln(\frac{S_0}{H})}{\sigma\sqrt{T}} + m\sigma\sqrt{T}.
\end{aligned}
$$

Then, depending on the relationship between the barrier and the strike price, we have:

Barrier Type	Pricing Formula for Continuously Monitored Option
Call, $H \leq K$	
down-in(DI)	$S_0 e^{-\delta T}(\frac{H}{S_0})^{2m} N(y) - K e^{-rT}(\frac{H}{S_0})^{2m-2} N(y - \sigma\sqrt{T})$
down-out(DO)	$C_{BS} - C_{DI}$
up-in(UI)	C_{BS}
up-out(UO)	0
Put, $H \leq K$	
down-in	$-S_0 e^{-\delta T} N(-x) + K e^{-rT} N(-x+\sigma\sqrt{T}) + S_0 e^{-\delta T}(\frac{H}{S_0})^{2m}(N(y) - N(z)) - K e^{-rT}(\frac{H}{S_0})^{2m-2}(N(y - \sigma\sqrt{T}) - N(z - \sigma\sqrt{T}))$
down-out	$P_{BS} - P_{DI}$
up-in	$P_{BS} - P_{UO}$
up-out	$-S_0 e^{-\delta T} N(-x) + K e^{-rT} N(-x + \sigma\sqrt{T}) + S_0 e^{-\delta T}(\frac{H}{S_0})^{2m} N(-z) - K e^{-rT}(\frac{H}{S_0})^{2m-2} N(-z + \sigma\sqrt{T})$
Call, $H > K$	
down-in	$C_{BS} - C_{DO}$
down-out	$S_0 e^{-\delta T} N(x) - K e^{-rT} N(x - \sigma\sqrt{T}) - S_0 e^{-\delta T}(\frac{H}{S_0})^{2m} N(z) + K e^{-rT}(\frac{H}{S_0})^{2m-2} N(z - \sigma\sqrt{T})$
up-in	$S_0 e^{-\delta T} N(x) - K e^{-rT} N(x - \sigma\sqrt{T}) - S_0 e^{-\delta T}(\frac{H}{S_0})^{2m}(N(-y) - N(-z)) + K e^{-rT}(\frac{H}{S_0})^{2m-2}(N(-y + \sigma\sqrt{T}) - N(-z + \sigma\sqrt{T}))$
up-out	$C_{BS} - C_{UI}$
Put, $H > K$	
down-in	P_{BS}
down-out	0
up-in	$S_0 e^{-\delta T} N(x) - K e^{-rT} N(x - \sigma\sqrt{T}) - S_0 e^{-\delta T}(\frac{H}{S_0})^{2m}(N(-y) - N(-z)) + K e^{-rT}(\frac{H}{S_0})^{2m-2}(N(-y + \sigma\sqrt{T}) - N(-z + \sigma\sqrt{T}))$
up-out	$-S_0 e^{-\delta T}(\frac{H}{S_0})^{2m} N(-y) + K e^{-rT}(\frac{H}{S_0})^{2m-2} N(-y + \sigma\sqrt{T})$

Table E.1: Black-Scholes formulas for continuously monitored barrier options

Appendix F

Derivation of the Critical Values for CME Entropy

For simplicity in notation, we temporarily ignore the subscript t in the problem, which in no way affects the validity of the derivation. We have objective function:

$$H(S^1) = -\lambda S^1 \ln(\lambda S^1) - (S - \lambda S^1) \ln(S - \lambda S^1),$$

with first derivative:

$$H'(S^1) = -\lambda \ln(\lambda S^1) + \lambda \ln(S - \lambda S^1).$$

Thus, the first order optimality conditions imply:

$$H'(S^1) = 0 \Rightarrow \lambda S^1 = S - \lambda S^1 \Rightarrow \hat{S^1} = \frac{S}{2\lambda}.$$

Therefore, by equation (3.26), we get:

$$\hat{S^2} = \frac{S}{2(1-\lambda)}.$$

Now, check second-order condition (convexity), we have:

$$H''(S^1) = -\frac{\lambda}{S^1} - \frac{\lambda^2}{S - \lambda S^1} \Rightarrow H''(\hat{S^1}) = \frac{-4\lambda^2}{S} < 0.$$

Therefore, the results are just as we proposed in Section 3.3.1.

References

[1] Kapadia N. Bakshi, G. and D. Madan. Stock return characteristics, skew laws, and the differential pricing of individual equity options. *The Review of Financial Studies*, 16:101–143, 2003.

[2] F. Black and M. Scholes. The pricing of options and corporate liabilities. *Journal of Political Economy*, 1973.

[3] P. Boyle. Options: a monte carlo approach. *Journal of Financial Economics*, 4:323338, 1997.

[4] D. Brigo and F. Mercurio. Lognormal-mixture dynamics and calibration to market volatility smiles. *International Journal of Theoretical and Applied Finance*, 5(4):427–446, 2002.

[5] C. Brown and R. David. Skewness and kurtosis implied by option prices: A correction. *Journal of Financial Research*, 25(2):279–282, 1995.

[6] D. Cassidy, M. Hamp, and R. Rachid. Pricing european options with a log students t-distribution: A gosset formula. *Physica A Statistical Mechanics and its Applications*.

[7] K. Chen and Y. Lyuu. Accurate pricing formulas for asian options. *Applied Mathematics and Computation*, 188(2), 2007.

[8] D. Chiras and S. Manaster. The information content of prices and a test of market efficiency. *Journal of Financial Economics*, 1978.

[9] R. Cont and José da Fonseca. Dynamics of implied volatility surfaces. *Quantitative Finance*, 2:45–60, 2002.

[10] C. Corrado and T. Su. Implied volatility skews and stock index skewness and kurtosis implied by S&P500 index option prices. *Journal of Financial Research*, 1996.

[11] C. Corrado and T. Su. Implied volatility skews and stock return skewness and kurtosis implied by stock option prices. *The European Journal of Finance*, 1997.

[12] T. Daglish, J. Hull, and W. Suo. Volatility surfaces: theory, rules of thumb, and empirical evidence. *Quantitative Finance*, 7(5):507–524, 2007.

[13] J. Duan. The GARCH option pricing model. *Mathematical Finance*, 5(1):13–32, 1995.

[14] B. Dupire. Pricing with a smile. *Risk*, 7:28–20, 1994.

[15] R. Engle and C. Mustafa. Implied arch models from options prices. *Journal of Econometrics*, 52(1-2):289–311, 1992.

[16] C. Gourieroux and A. Monfort. Econometric specification of stochastic discount factor models. *Journal of Econometrics*, 136, 2005.

[17] M.R. Hardy. A regime switching model of long term stock returns. *North American Actuarial Journal*, 5(1), 2001.

[18] L. Harris. Transactions data tests of the mixture of distributions hypothesis. *Journal of Financial and Quantitative Analysis*, 22(2), 1987.

[19] J.M. Harrison and D. Kreps. Martingales and arbitrage in multiperiod securities markets. *Journal of Economic Theory*, 20:381–408, 1979.

[20] J.M. Harrison and S. Pliska. Martingales and stochastic integrals in the theory of continuous trading. *Stochastic Processes and their Applications*, 11:215–260, 1981.

[21] E. Haug. *The Complete Guide to Option Pricing Formulas*. McGraw-Hill Professional, 2007.

[22] S. Heston. A closed-form solution for options with stochastic volatility with applications to bond and currency options. *Review of Financial Studies*, 6:237–243, 1993.

[23] J. Hull and A. White. The pricing of options on assets with stochastic volatilities. *Journal of Finance*, 42:281–300, 1987.

[24] J. Hull and A. White. Efficient procedures for valuing european and american path-dependent options. *Journal of Derivatives*, 1:21–23, 1993.

[25] K. Jacobs and L. Karoui. Conditional volatility in affine term-structure models: Evidence from treasury and swap markets. *Journal of Financial Economics*, 91:288–318, 2009.

[26] N. Ju. Pricing asian and basket options via taylor expansion. *Journal of Computational Finance*, 5(3), 2002.

[27] S.G. Kou. On pricing of discrete barrier options. *Statistica Sinica*, 13:955–964, 2003.

[28] D. Leisen. Mixed lognormal distributions for financial applications. Technical report, 2003.

[29] D. Leisen. Mixed lognormal distributions for derivatives pricing and risk-management. Computing in Economics and Finance 2004 48, Society for Computational Economics, August 2004.

[30] F. Longstaff. Option pricing and the martingale restriction. *Review of Financial Studies*, 8(4):1091–1124, 1995.

[31] S. Markose and A. Alentorn. Option pricing and the implied tail index with the generalized extreme value(GEV) distribution. Computing in Economics and Finance 397, Society for Computational Economics, 2005.

[32] W. Melick and C. Thomas. Recovering an asset's implied pdf from option prices: An application to crude oil during the gulf crisis. *Journal of Financial and Quantitative Analysis*, 32(1):91–115, 1997.

[33] R. Merton. Theory of rational option pricing. *The Bell Journal of Economics and Management Science*, 4(1), 1973.

[34] R. Merton. Option pricing when underlying stock returns are discontinuous. *Journal of Financial Economics*, 3(1-2):125–144, 1976.

[35] M. Neumann. Option pricing under the mixture of distributions hypothesis. *Preliminary Discussion Paper*, 2002.

[36] E. Reiner and M. Rubinstein. Breaking down the barriers. *Risk*, 4(8), 1991.

[37] M. Rubinstein. Implied binomial trees. *The Journal of Finance*, 49(3):771–818, 1994.

[38] M. Rubinstein and J. Jackwerth. Recovering probability distributions from option prices. *The Journal of Finance*, 51(5):1611–32, 1996.

[39] W. Schoutens and S. Symens. The pricing of exotic options by monte-carlo simulations in a Lévy market with stochastic volatility. *International Journal of Theoretical and Applied Finance*, 6(8):839–864, 2003.

[40] D. Shimko. Bounds of probability. *Risk*, 6(4):33–37, 1993.